The Astron Astrophys Rev (1994) 5:293–331

THE
ASTRONOMY
AND
ASTROPHYSICS
REVIEW

Kinematical properties of early-type galaxies

Massimo Capaccioli[1,2] **and Giuseppe Longo**[1]

[1] Osservatorio Astronomico di Capodimonte, via Moiariello 16, I–80131 Napoli, Italy
[2] Dipartimento di Astronomia, Università di Padova, Vicolo dell'Osservatorio 5, I–35122 Padova, Italy

Received April 19, 1994

Summary. In the last decade, our understanding of early-type galaxies has greatly changed: from rather uninteresting oblate spheroids flattened by rotation to multicomponent stellar systems whose structure, formation mechanisms, and evolution, are far from being understood. This new scenario is mainly the consequence of the huge growth, in quantity and in quality, of kinematical data obtained from high signal to noise spectral data. Rotation curves and velocity dispersion profiles extending out to almost 2 effective radii are now available, together with line asymmetry measurements, for the stellar components of a fairly large sample of galaxies. For a few galaxies, outer halo tracers such as globular clusters and/or planetary nebulae allow to explore the kinematics out at $4 \sim 6r_e$. In this article we focus on these data giving particular emphasis on the most recent results. Reference is given to other review articles complementing the approach presented here.

Key words: Galaxies: elliptical – Galaxies: kinematics and dynamics of – Galaxies: structure of

Preamble

It is common practice to name *early-types* a heterogeneous collection of galaxy–types comprising ellipticals, lenticulars, and, by an un-written rule, also bulges of spirals. Such a convention, inspired by morphological analogies and by similarities in the shapes of the surface brightness profiles, is now shaking under new photometric and kinematical evidence at all wavelengths. For this reason, and unless explicitly noted, all results presented here refer to ellipticals and are not necessarily applicable to bulges too.

Correspondence to: M. Capaccioli

Albeit this review is committed to kinematical observations, neither photometric properties nor dynamical models can be completely ignored. The existence of a synergic relationship between kinematics and dynamics makes the borderline between these two branches of the extragalactic research necessarily fuzzy: all the observational quantities are of kinematical nature and most, if not all, of the interesting conclusions are dynamical. Furthermore, the modeling of spheroidal and, even worse, of triaxial systems is a highly undetermined problem, and both kinematical and photometric data must be combined to constrain the models.

Exhaustive reviews of the properties of early-type systems have recently appeared (Nieto 1988; Kormendy and Djorgovski 1989; Bender 1990a; Franx 1990, 1992; de Zeeuw and Franx 1991, Capaccioli and Caon 1992, Bertin and Stiavelli 1993, Djorgovski 1993, 1994), and meetings have been in part or fully devoted to the topic: de Zeeuw (1987), Wielen (1990), Longo et al. (1992), Merritt (1992), Danziger et al. (1993a).

The paper is organized as follows. Section 1 retraces the key perceptions which combined to shape our present understanding of early-type galaxies, and Sect. 2 illustrates which quantities can be derived from spectroscopic observations. Sect. 3 is a quick presentation of the state-of-the-art kinematical data and Sect. 4 of the principal reduction techniques. In Sects. 5, 6, and 7, the kinematical measurements are regarded as tools for probing the intrinsic structure of galaxies, while the kinematics of the outer regions is analysed in Sect. 8. The correlations between kinematical and global properties are discussed in Sect. 9.

1 Introduction

Still in the early Seventies, the kinematical properties of early-type galaxies were virtually unknown, even though many later discoveries had been anticipated in a few seminal papers (e.g. van Houten 1961). A few central velocity dispersions had been measured by Minkowski (1961) and others, but not much work was going on in the field, the dominant factor preventing any real progress being the endemic lack of strong and/or extended emission lines in the spectra of early-type galaxies. In fact, differently from most late-type galaxies, these systems are on average gas poor. As a consequence, their kinematics must be inferred from stellar absorption features, which are difficult to detect and to measure, and which provide results difficult to model.

A second factor was more of a psychological nature. The existence of scale-free formulae, such as the so-called $r^{1/4}$ law (de Vaucouleurs 1948a-b, 1953), matching the surface brightness profiles of almost all ellipticals and bulges of lenticulars and spirals (Capaccioli 1989, but see also Caon et al. 1993), had nourished the feeling that these objects form a homogeneous and rather uninteresting family of oblate spheroids flattened by rotation about their polar axis, which could be described in terms of a fluid–dynamical approximation (Freeman 1975, Gott 1975, Larson 1975, Wilson 1975). This widespread belief came suddenly to an end when Bertola and Capaccioli (1975) showed that NGC 4697, a galaxy classified as E5 at the time (but see Capaccioli 1987), rotates far too slowly to account for its observed flattening. Soon after, Illingworth (1977) confirmed this finding in a larger sample of objects. Binney (1976) considered the anisotropy of the velocity dispersion tensor as a possible flattening mechanism: gravitational forces being compensated by gradients in the velocity dispersion tensor. By relaxing the hypothesis of oblateness, Binney opened the way to the triaxial models, strongly invoked also by the re-discovered isophotal

'twisting' (Barbon et al. 1976; King 1978, Williams and Schwarzschild 1979, Leach 1981), already seen by Liller (1960, 1966). Binney also introduced the so-called anisotropy parameter $(V/\sigma)^*$ as a tool to probe the intrinsic structure of ellipticals; this is the ratio between the maximum rotational velocity V_{max} and the central velocity dispersion σ_0, measured in units of the value expected for an isotropic rotator of the same apparent flattening. Davies et al. (1983) found that $(V/\sigma)^*$ correlates with the absolute magnitude of ellipticals, thus showing, for the first time on objective grounds, that the E class encompasses at least two families – low and high luminosity –, having distinct kinematical properties.

Another breakthrough took place in the field when it was realised that interactions and secondary evolution play an important role in fixing the present observed structure of ellipticals (Toomre 1977). The discovery of faint shell-like structures (Malin 1979), of kinematically decoupled cores (Franx and Illingworth 1988), of anomalous blue colors (Zepf et al. 1991), of counter-rotating dust lanes and gaseous disks (Bertola et al. 1985), and of narrow polar rings (Whitmore et al. 1990), clearly indicate that cannibalism and merging are recent history for at least some ellipticals.

The third milestone was laid when de Vaucouleurs and Capaccioli (1979), in stating that the light profile of the standard elliptical NGC 3379 is well matched by the $r^{1/4}$ formula over a range of more than 10 magnitudes, noticed the existence of faint systematic deviations from the smooth interpolation (*'ripples'*), and suggested that they could be the photometric signature of a faint underlying structure (cf. Capaccioli et al. 1990a for a photometric re-classification of this classical E galaxy). Detailed photometric studies identified these subcomponents as weak disks (Capaccioli 1987, Carter 1987, Jedrzejewski 1987). A powerful tool to study these weak structures is the isophotal shape analysis (e.g. Lauer 1985, Capaccioli et al. 1990b), particularly through the parameter a_4/a (Bender and Möllenhoff 1987), where a_4 is the 4-th cosine coefficient in the Fourier expansion of the radial residuals of an isophote from its best fitting ellipse with semimajor axis length a. Ellipticals having $a_4/a > 0$ are named *'disky'* for their resemblance to weak-disk galaxies, and those with $a_4/a < 0$ *'boxy'*. The parameter a_4/a was soon discovered to correlate with the internal kinematics, disky ellipticals being mostly rotationally flattened and boxy E's being predominantly supported by the anisotropy of the velocity dispersion (Bender 1988a, Bender et al. 1989, Nieto et al. 1988).

The fourth and last discovery was that, in spite of a great variety in the detailed structure and non-optical properties, spheroidal systems have a quite regular overall behaviour and populate a two dimensional manifold in the space defined by their central velocity dispersion, central surface brightness, and effective radius (Brosche 1973, Faber et al. 1987, Djorgovski and Davis 1987). The existence of a *'fundamental plane'*, even though not yet fully understood, has been interpreted as the signature of similar formation histories (Burstein et al. 1993, and references therein). On the other hand, the presumed 'universality' of the $r^{1/4}$ law seems now more an artifact of the small radial interval over which the fit of the luminosity profile is performed: over larger ranges, still unexplained systematic deviations are present which appear to correlate with the total luminosity (Caon et al. 1993). The few cases of fine matching of the $r^{1/4}$ law over the full surface brightness interval covered by deep observations (e.g. NGC 3379) are interpreted as due to the filling of the 'concave' (in $r^{1/4}$ units) light profile of a bulge with the exponential profile of a disk (Capaccioli 1987).

It is now clear that the apparent simplicity of early-type galaxies is highly deceptive; they are instead complex, multicomponent systems whose present structure, formation mechanisms, and evolution are not yet fully understood. Rather than the

properties of distinct galaxian types, this new scenario leads us to analyse those of the (close to) spheroidal, mainly pressure supported stellar systems (also known as *'hot'* stellar systems), which are harbored in most galaxies (except the irregular galaxies and possibly the extreme disk–systems).

2 The kinematical observables

The two body relaxation time for a dynamically 'hot' stellar system is given by:

$$\tau_{rel} \simeq \frac{\sigma^3}{G^2 m^2 n \log \Lambda} \tag{1}$$

where σ is the stellar velocity dispersion (see below), n is the star density number, m is the average star mass, and Λ is the Coulomb Logarithm, $\Lambda \simeq R\sigma^2/Gm$ (Binney and Tremaine 1987, p. 190), R is the galaxy characteristic radius and G is the constant of gravity. Since a typical elliptical has $\tau_{rel} \sim 10^{14}$ yr, it can be fairly modeled as a collisionless system. By neglecting the interactions between individual stars, the forces acting on stars are functions of the galaxian potential $\Phi(\mathbf{x}, t)$ only. It follows that:
(i) gravitational accelerations are independent of the mass and stars can be assumed to be equal mass particles (Bertin and Stiavelli 1993);
(ii) given the large number of particles involved, the dynamical state of a galaxy is completely specified by the phase space density of the stars, also known as distribution function $f = f(\mathbf{x}, \mathbf{v}, t)$, which gives the relative number of stars having, at the time t, position $\mathbf{x}$ and velocity $\mathbf{v}$.

The lowest order moments of f obey the well known Jeans equation (for a detailed exposition see Chapter IV in Binney and Tremaine 1987):

$$\frac{\partial \overline{v_j}}{\partial t} + \overline{v_i}\frac{\partial \overline{v_j}}{\partial x_i} = -\rho\frac{\partial \Phi}{\partial x_j} - \frac{\partial(\rho\sigma_{ij}^2)}{\partial x_i} \tag{2}$$

where $\rho \equiv \int f\, d^3\mathbf{v}$ is the spatial density, $\overline{v_i} \equiv \frac{1}{\rho}\int f\, v_i\, d^3\mathbf{v}$ the mean stellar velocity, and $\sigma_{ij}^2 \equiv \overline{v_i v_j} - \overline{v_i}\,\overline{v_j}$ the velocity dispersion tensor. Φ and f are unknown functions of the quantities $\overline{\mathbf{v}}$, σ and ρ, which, under some restricting hypotheses, can be constrained by observations.

On the observational side, information on the dynamical state of unresolved stellar systems is derived from projected quantities, that is by quantities which are integrated along the line of sight: the surface brightness profile $\mu(r_p) = -2.5\ \log I(r_p)$ at the projected galactocentric radius r_p, picturing the radial run of the luminous mass distribution, and the spectral line profile $b_p(\lambda, r_p)$. Therefore it does not take us by surprise that, even in an ideal case, the problem of constraining the dynamical state of a stellar system on the basis of observed quantities is strongly underdetermined (see the outstanding review by Merritt 1993).

A most effective example of the indetermination of dynamical models has been given by Binney and Mamon (1982) for the simple case of a spherical, non-rotating galaxy in steady state. By rewriting Eq. 2 in spherical coordinates and by considering that $\overline{v_r} = 0$ (steady-state), and $\overline{v_\theta^2} = \overline{v_\phi^2}$ (null rotation), we obtain:

$$\frac{1}{\rho}\frac{d(\rho\overline{v_r^2})}{dr} + 2\,\beta\frac{\overline{v_r^2}}{r} = -\frac{d\Phi}{dr} \tag{3}$$

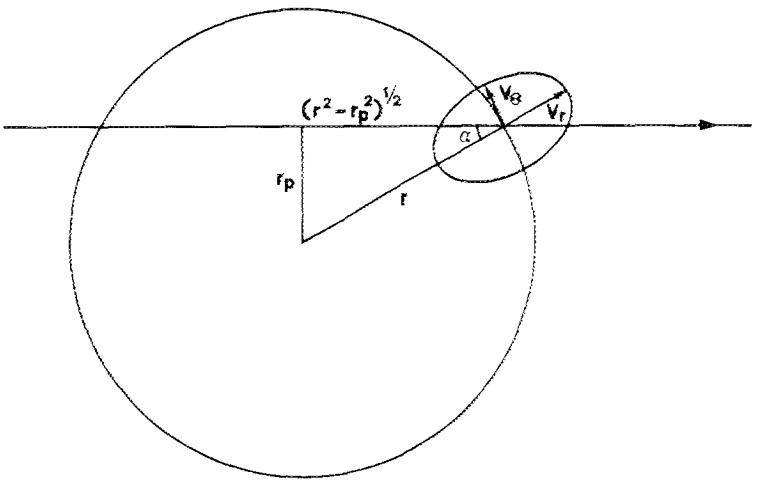

Fig. 1. Geometry assumed in the computations

where $\beta(r) \equiv 1 - \left(\overline{\sigma_\theta^2}/\overline{\sigma_r^2}\right)$ is the so-called anisotropy parameter and σ_θ and σ_r are the tangential and radial velocity dispersion, respectively.

In the absence of independent constraints on β, Eq. 3 can be solved in both the isotropic ($\beta = 0$) and the anisotropic ($\beta \neq 0$) cases, leading to completely different results. In other words, the same surface brightness and velocity dispersion profiles can be modeled either by making assumptions on the degree of anisotropy and then deriving the potential, or by making assumptions on the potential and deriving the degree of anisotropy (cf. Binney and Tremaine 1987, pag. 203).

A different type of uncertainty arises from the non-trivial link existing between the observed spectral line profiles and the derived quantities. Line profiles are usually affected by:
(i) geometrical factors: inclination of the rotation axis and non-trivial integration of the spatial information along the line of sight;
(ii) instrumental factors: finite spectral resolution and spectral window of the data;
(iii) noise: especially present in the wings of absorption features.

All the above factors order moments of the distribution function from $b_p(\lambda, r_p)$ (Binney and Mamon 1982).

Lacking clearly identifiable symmetry planes, the inclination of the rotation axis with respect to the line of sight must be inferred or constrained by indirect evidence such as, for instance, the orientation of dust lanes and gaseous disks, or the detailed study of the velocity field (Tenjes et al. 1993). Unfortunately – owing to the scarcity of observing time associated to the need of prompt results – in most cases the velocity field is sampled at one or two position angles only, and specifically tailored instruments such as TIGER (Courtes et al. 1988) are still in their infancy.

Integration along the line of sight can be partially corrected by making some assumptions on the properties of the system (Capaccioli 1973, Busarello et al. 1992). This is, however, a tricky procedure; even in the simple case of a spherical, non-rotating, isotropic galaxy (see Fig. 1), it is:

$$I(r_p) = 2 \int_{r_p}^{\infty} \frac{\ell(r)\, r\, dr}{\sqrt{r^2 - {r_p}^2}} \tag{4}$$

$$I(r_p)\, \sigma^2(r_p) = 2 \int_{r_p}^{\infty} \frac{\ell(r)\, \overline{v_r^2(r_p)} r\, dr}{\sqrt{r^2 - {r_p}^2}} \tag{5}$$

These Abel integral equations can be inverted analytically, obtaining:

$$\ell(r) = -\frac{1}{\pi} \int_{r}^{\infty} \frac{dI}{dr_p} \frac{dr_p}{\sqrt{{r_p}^2 - r^2}} \tag{6}$$

$$\ell(r)\overline{v_r^2}(r) = -\frac{1}{\pi} \int_{r}^{\infty} \frac{d(I\,\sigma^2)}{dr_p} \frac{dr_p}{\sqrt{{r_p}^2 - r^2}} \tag{7}$$

but the presence of derivatives makes the above formulae very sensitive to the level of noise in I and σ^2 (Merritt 1993).

A new observational tool to probe the dynamical structure of 'hot' galaxies has been secured by Dejonghe (1987a) and others (Sect. 4) who, by studying the line profiles resulting from anisotropic Plummer's models, have shown that radial variations of β result in an appreciable distortion of the line profile.

3 State-of-the-art of the kinematical information

The current revolution in our understanding of 'hot' stellar systems has been triggered also by the improved technology of optical observations and of their reduction: digital detectors and modern image processing facilities have fostered an impressive growth in the amount and quality of the data. A recent compendium by Busarello et al. (1994b) reports 1692 central velocity dispersions, 986 rotation curves, and 561 velocity dispersion profiles, to be compared to fewer than 30 central velocity dispersions quoted by Capaccioli in 1979. Other valuable kinematical tools besides optical lines – usually in absorption – are HI and CO emission lines: a type of observation which, despite the small amount of both atomic and molecular gas present in early-type systems, is steadily increasing in quality and number of positive detections (Roberts et al. 1991). X–ray observations, which were thought to be a powerful probe of the kinematics of the outer halo, have been shown to be practically useless for this purpose (Bertin 1993).

We shall first concentrate on the kinematical data obtained from stellar absorption features measured along the projected major axis. Lenticular galaxies have rotation curves similar to those of later morphological type objects; they are characterized by a sharp rise up to a first maximum, followed by a dip and then by a shallower rise (Capaccioli 1979). This dip is the signature of the transition between disk-dominated and bulge-dominated regions of the galaxy (Fig. 2a). In the case of *'bona fide'* ellipticals, it can help discriminating on a kinematical basis between truly diskless systems and misclassified lenticulars. On the average, ellipticals have shallower and featureless rotation curves (Fig. 2b). Most objects have symmetric rotation curves, even though noticeable exceptions are known (Fig. 2c). In some cases the distortions are explained by the presence of strongly interacting nearby companions (Fig. 2d).

Most of the rotation curves available in the literature do not extend far enough to ensure that the maximum rotational velocity has been reached, and, in the majority

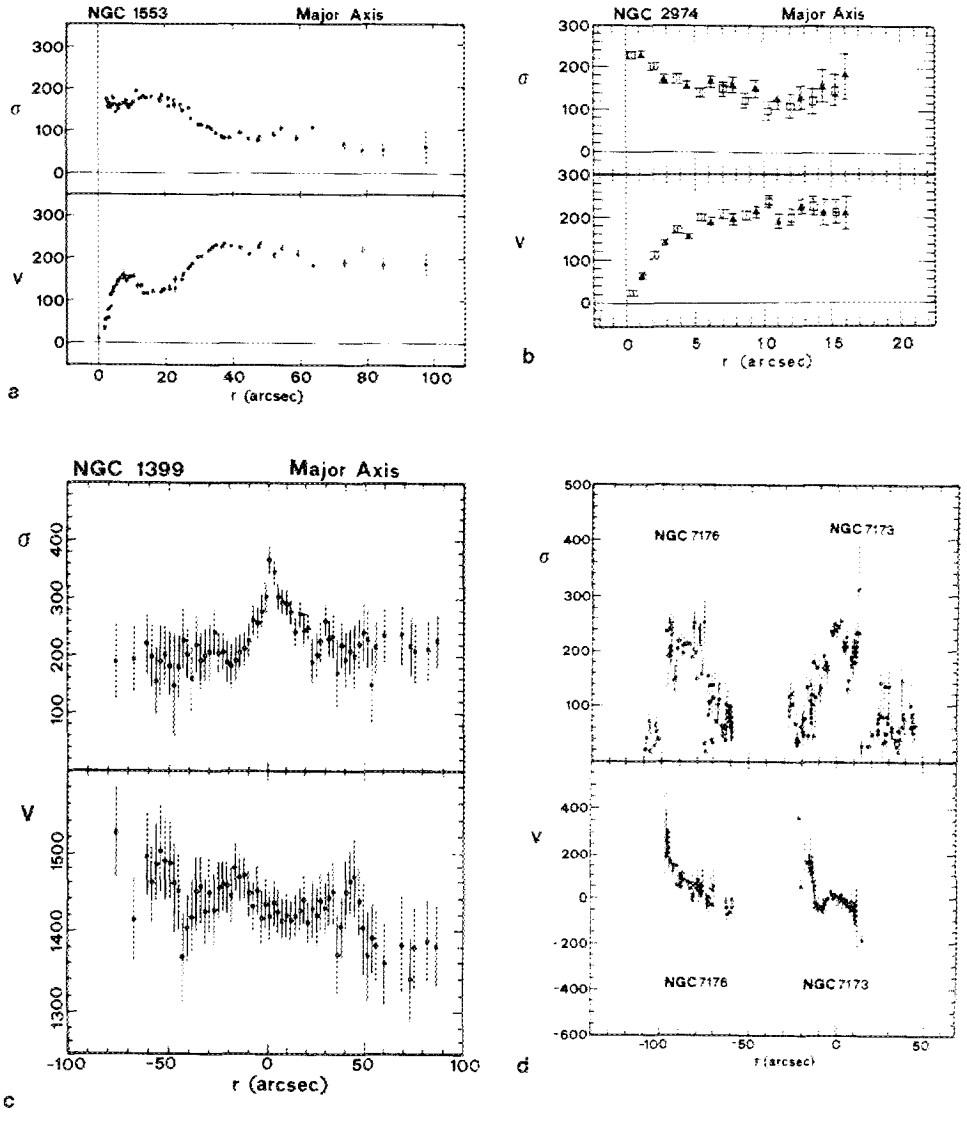

Fig. 2. Velocity dispersion profiles and rotation curves along the major axis for some early-ty
a NGC 1553, an S0 seen under a favourable inclination (from Kormendy 1984a). **b** NGC 2974, a
E4 with mildly pointed isophotes (from Cinzano and van der Marel 1993). **c** NGC 1399, an E galaxy with
a high degree of anisotropy (from Bicknell et al. 1989). **d** The interacting pair of ellipticals NGC 7173 and
7176 in the compact group Hickson 90 (from Longo et al. 1993)

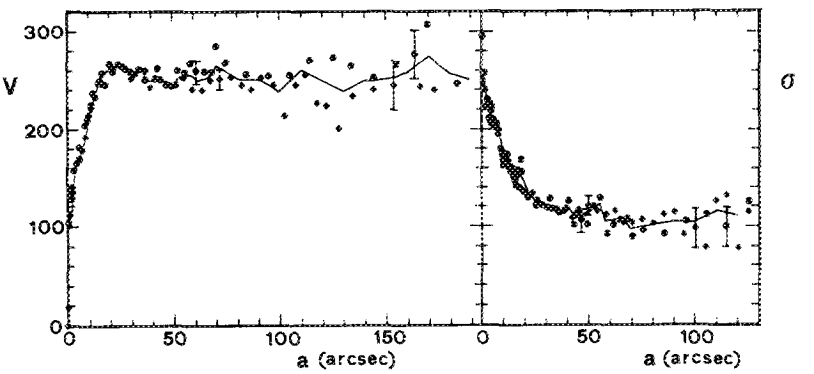

Fig. 3. Extended rotation curve (left) and velocity dispersion profile (right) for the edge-on lenticular NGC3115 (from Capaccioli et al. 1993a; $r_e \simeq 50''$)

of the cases, the measurements are confined within one effective radius r_e, i.e. inside the isophote encircling half of the total light of the galaxy. Only very recently, better detectors and improved reduction procedures have allowed to reach galactocentric distances as large as $2.0 \sim 2.5 r_e$ (Sect. 8 and references therein, and Fig. 3), showing that the rotation curves remain flat out to the last measured point. The restrictions to the radial range apply in particular to the velocity dispersion measurements which require values of the signal-to-noise ratio (S/N) typically ~ 6 times higher than for the rotational velocities (Franx et al. 1989).

On average, the velocity dispersion profiles of lenticulars reach a central value similar to that of normal ellipticals: the sample of Busarello et al. (1994b) gives $\langle \sigma_0 \rangle (S0) = 205 \pm 15$ km s^{-1}, to be compared with 217 ± 12 for the ellipticals.

Even though quite recent and successfully applied to a handful of objects only, the analysis of the shapes of the line profiles has already led to exciting results, such as the detection of dynamical subcomponents (Franx and Illingworth 1988) and of velocity anisotropies. Unfortunately, the effects of anisotropy on line profiles, which demand $S/N \geq 10$ to be measurable (Rix and White 1992), are better disentangled at relatively large radii (i.e. $r \geq 1 \sim 1.5 r_e$), due to the smearing in the inner and denser galaxian regions. Now, the required signal-to-noise ratio is not easily achieved in early-type galaxies, where the sharp decrease of the surface brightness with the radius makes the absorption features – and especially their wings – very noisy.

In conclusion, so far the kinematics of early-type galaxies derived from high S/N long-slit spectra is capable of providing the radial run of the rotational velocity and velocity dispersion of the stellar component integrated along the line of sight out to $\simeq 2 \sim 3\ r_e$. The asymmetry of the line profiles can be measured out to $\simeq 1.5 \sim 2\ r_e$.

Because so little gas is present in early-type galaxies, emission lines (both in the optical and radio ranges) are not of much help in pushing kinematical sampling out to large galactocentric distances. Atomic gas emission (as detected from the HI line) comes usually from a disk or ring hidden in the inner galaxy regions, while molecular gas (from the CO line) is centrally peaked (van Gorkom 1992, and references therein). The decoupling of the gaseous from the stellar component (see Sect. 7.3) requires additional hypotheses which render the gas a useful tool to probe the intrinsic structure of early-type galaxies, but undermines its use as kinematical probe.

4 Data reduction techniques for absorption line data

Let us put $x = \log \lambda$, and let $b(x)$ indicate the broadening function[1] (hereafter =BF), i.e. the intrinsic profile of the spectral line which would be observed under ideal conditions (infinitely thin slit and outside of the atmosphere), $g_{obs}(x)$ the observed galaxy spectrum, and $t(x)$ the spectrum of a template star assumed to mimic that of the galaxy. Then,

$$g_{obs}(x) = \gamma \times \left[t(x) * b(x - x_r)\right] + \epsilon(x) \tag{8}$$

where x_r represents the contribution from the rotation of the galaxy, $\epsilon(x)$ is the error intrinsic to the model, and γ is a scaling factor, also called *'line strength'*. In the presence of noise, the inversion of the above equation poses a non-trivial problem.

All methods assume that $b(x)$ can be represented by means of parameterized functions. Older ones usually postulate that it is a Gaussian,

$$b(V) = \frac{1}{\sigma\sqrt{2\pi}} \exp\left[-\frac{(V - V_0)^2}{2\sigma^2}\right] \tag{9}$$

and differ mainly in the strategies adopted to retrieve the three parameters γ, V_0, and σ.

Actually, isotropic models lead to substantially Gaussian line profiles and this turns out to be a good approximation for many – but not all – objects. For instance, Dressler (1984) has shown that the line of sight velocity distribution of NGC 221 is Gaussian within 1%. Similar results have been reached by Winsall and Freeman (1993) for the outer regions of four luminous ellipticals (NGC 1399, 1404, 4472, 4486).

In the following paragraphs we will briefly describe the most relevant techniques for reducing absorption–line spectral data.

4.1 Pre–history

In the early methods V and σ were measured independently one from the other. The rotation curve was obtained by setting visually the minima of the absorption lines (cf. Bertola and Capaccioli 1975). The measurement of the velocity dispersion was based on the visual comparison of the galaxy spectrum with an artificially broadened template spectrum, a technique highly subjective and unreliable in the presence of noise. The template spectra were broadened directly at the telescope by exposing the star through semitransparent slit jaws, or in the darkroom (Minkowski 1954, 1961), or by numerically convolving the observed spectra with Gaussians of different widths (Burbidge et al. 1961a,b,c; Richstone and Sargent 1972). The latest and most refined implementations of a visual method were by Morton and collaborators (1972, 1973, 1976). Faber and Jackson (1976) compared the spectra of the galaxy and of the template in the Fourier transformed space. Due to their high degree of subjectivity, visual methods were rapidly superseded by other techniques.

[1] The change of variable implies $dx = d\lambda/\lambda$ or, according to the Doppler formula, $dx = dv/c$: that is, dx is proportional to the velocity shift. This allows to represent b as a Gaussian of constant width, independently of the wavelength

4.2 The recent past

4.2.1 The Fourier Quotient Methods (FQ)

The first truly non-subjective method is the *Fourier Quotient*, originally suggested by Brault and White (1971) and by Simkin (1974), and implemented by Sargent et al. (1977). Successive and slightly different implementations are those by Dressler (1979), also known as *Fourier Difference* (= FD), by Davies (1981), by Larsen et al. (1983), and by Franx et al. (1989; also known as *Fourier Fitting*). These later versions of the FQ differ mainly in the treatment of the noise but, as shown by Larsen et al. (1983), they give equivalent results and can be treated as a unique family.

The retrieval of the BF in the FQ–based methods is founded on the *'convolution theorem'*: the Fourier transform of $g(x)$ is divided by that of $t(x)$ and the result is back-transformed. Let us denote the Fourier–transformed quantities with capital letters. The BF, modelled as a Gaussian:

$$B(k) = \gamma \exp\left[-\frac{1}{2}\left(\frac{2\pi k\sigma}{N}\right) + \left(\frac{2\pi v i k}{N}\right)\right] \tag{10}$$

where N is the number of wavelength bins (in $ln\lambda$), is fitted to the ratio $Q(k) \equiv G(k)/T(k)$, in order to determine the three free parameters v, σ, and γ. The best fit is usually obtained by minimizing the ratio:

$$\chi^2 = \sum_{k=k_1}^{k_2} \left| \frac{Q(k) - B(k)}{\Delta Q(k)} \right|^2 \tag{11}$$

The limits k_1 and k_2 exclude low and high frequency variations which are not expected to be a property of the BF, and $\Delta Q(k)$ is the expected uncertainty in $Q(k)$. The strength of the method rests on the fact that, by dividing $G(k)$ by $T(k)$, the instrumental effects are removed or, in practice, minimized.

Even though very effective in dealing with relatively noisy data, the FQ approach has however several shortcomings. Extensive tests of the method lead to the following considerations (Ferrario 1990, and references therein):

(i) it cannot be applied to non-Gaussian BF's;

(ii) the errors in the FQ are strongly correlated and cannot be estimated in a reliable way. It should also be noticed that, in the early implementations of the code, errors were overestimated by a factor $\sqrt{2}$ (Franx et al. 1989);

(iii) σ is very sensitive to small differences in the metallicities of the galaxy and of the template. In fact, the BF is derived through a fit in the Fourier space, where absorption features from all parts of the spectrum interact with each other (Laird and Levison 1985);

(iv) if the velocity dispersion is close to the instrumental resolution, the results are unreliable (Kormendy and Illingworth 1982).

4.2.2 Cross Correlation Methods (CC)

First introduced by Simkin (1972, 1974), the CC method was originally tailored for the radial velocity measurements only. It was then adapted to measure velocity dispersions by Tonry and Davis (1979). Modified versions have been proposed by

Larsen et al. (1983), also known as *Autocorrelation Method*, by Bottema (1988), by Dalle Ore et al. (1991), and by Franx et al. (1989).

In the CC method $g(x)$ and $t(x)$ are correlated as a function of the relative wavelength shift. The position of the highest peak gives the mean (or bulk) velocity. The velocity dispersion is then estimated by subtracting the width of the squared autocorrelation function of the template from the width of the cross-correlation peak. Dalle Ore et al. (1991) proposed a modified version of the CC method which, although never tested, is potentially capable of dealing with asymmetric BF's.

In comparison with the FQ, the CC method allows a more formal evaluation of the errors. Moreover:
(i) it is less dependent on metallicity differences between the galaxy and the template spectra, since the features used are only those in common to the galaxy and template spectra;
(ii) it is reliable also for values of σ smaller than the instrumental resolution (Bottema 1988);
(iii) it is completely insensitive to non-white noise (Dalle Ore et al. 1991);
(iv) its results are much less dependent on the S/N ratio of the template (Bottema 1988), for no quotient has to be performed.

The autocorrelation method correlates the two sides of the galaxy spectrum opposite to the center. It has the disadvantage of requiring the rotation curve to be symmetric. Not much literature is available on the method, but Davoust et al. (1985) noticed that the velocity values provided by the autocorrelation method are systematically lower than those derived by other methods.

4.2.3 Fourier Correlation Method (FCM)

FCM was first introduced by Bender (1990b) to solve some of the problems encountered by the standard CC approach. Its main characteristics are:
(i) higher accuracy than other methods in estimating the errors;
(ii) reliability of the velocity dispersion measurements even when σ is smaller than the spectral resolution;
(iii) little dependence of σ on the difference in metallicity between the template and the galaxy.

The FCM returns also an estimate of the asymmetry of the line profile (the gross effect of the asymmetry is to put more power in the imaginary part of the Fourier transform of the BF).

4.3 The present: line profile asymmetries

Let us now come back to the case of a spherical galaxy. If instrumental effects are neglected, then the line profile observed at the projected galactocentric distance x along the apparent major axis is:

$$b_x(v) = k \int_{-\infty}^{+\infty} \ell(r)\, \sigma(v^*)\, dy \tag{12}$$

where k is a constant, σ is assumed to be isotropic and independent of the radius, V is the rotational velocity, $v^* = \left(v - V(r)\frac{x}{r}\right)$, and $y^2 = r^2 - x^2$.

For a galaxy with a $r^{1/4}$ photometric profile, the light-density profile can be approximated by the Mellier and Mathez (1987) formula: $I(r) = I_c r^{-a} \exp\left(-br^{1/4}\right)$, where $a = 0.855$, $b = 7.6692$, and r is in units of the effective radius r_e.

For the sake of simplicity and in spite of its lack of physical meaning – the infinite wings of a Gaussian imply an infinite mass for the stellar system –, let us assume that σ is Gaussian (the Gaussian model for $b(x)$ implying that the galaxy is assumed to consist of one dynamical component only). Then,

$$b_x(v) = 2k \int_x^{+\infty} r^{1-a} \exp\left(-br^{1/4}\right) \times \times \exp\left(\frac{-\left[v - V(r)(x/r)\right]^2}{2\sigma_0^2}\right) \frac{dr}{\sqrt{r^2 - x^2}} \qquad (13)$$

If the rotational velocity is constant with radius, $V = V_0$ (fair assumption for $r \gtrsim r_e/4$), with simple arithmetic we obtain

$$b_x(v) = 2k \exp\left(\frac{-[v - V_0]^2}{2\sigma_0^2}\right) h(v; x, r_e, \sigma_0, V_0) \qquad (14)$$

i.e. the function h acts as a distortion on the Gaussian BF, here induced just by the integration along the line of sight. If $h \simeq$ const., as it is in our oversimplified model, then the center $V_x(obs)$ of the BF gives directly the value of the rotational velocity V at $r = x$ (after subtraction of the systemic velocity), and the standard deviation $\sigma_x(obs)$ measures the amount of random motions. Should one of the above assumptions be relaxed, then $b_x(v)$ might differ significantly from a simple Gaussian function. This may have consequences which are not just negative for us. In fact, even if the asymmetry of the BF implies a (model dependent) correction to recover the rotational velocity and the spatial velocity dispersion, on the other hand the study of the shape of $b_x(v)$ may disclose the nature and strength of the phenomena driving the distortion itself.

Since the early suggestion by Tonry (1984), the pioneering work by Dejonghe (1987a,b), and the first application by Franx and Illingworth (1988), much effort has been put in understanding and extracting the information contained in the observed line profiles.

Some effects are trivial to understand, such as, for instance, the asymmetry of the BF which is caused by a faint rapidly rotating cold component – a disk (Sect. 7.1) – hidden within a much brighter slowly rotating bulge (cf. Franx and Illingworth 1988, Bender et al. 1993).

Much more complex to model are the effects on the BF caused by the anisotropy of the velocity dispersion tensor which can introduce errors as large as 10% in the estimated rotational velocities and up to 30% in the central velocity dispersions (van der Marel and Franx 1993).

Gerhard (1993, but see also Winsall and Freeman 1993) has studied the effects produced on the line profile by anisotropy, steepness of the light density gradient, and shape of the potential well (by taking into account a Keplerian and a dark matter dominated – i.e. logarithmic – potential). His results can be summarized as follows: (i) deviations from purely Gaussian shape are easier to detect at large galactocentric distances where the smearing introduced by the line of sight integration is smaller;

(ii) strongly tangentially anisotropic distribution functions lead to an artificial flattening of the line profile (the effect depends on the stellar density profile, being larger for steep density gradients);
(iii) radially anisotropic distribution functions result in narrow line profiles with smaller velocity dispersions. The shape is close to Gaussian in Keplerian potentials and has extended wings in logarithmic potentials;
(iv) for steep density profiles, the BF reflects more a local average of the distribution function in the case of tangential anisotropy.

From the observational point of view, the retrieval of the true shape of the BF is undermined by various instrumental effects and especially by the noise in the wings of the absorption features, which makes it almost impossible to measure the higher order moments of the BF, $m_n = \int v^n b(v)\, d^3v$.

It is therefore a common practice to analyze the BF in terms of the deviations of the line profile from a purely Gaussian shape, and the various methods presented in the following paragraphs differ mainly in the way these deviations are parameterized. The physical meaning of the adopted parameters is then tested against predictions obtained from models.

4.3.1 Modified Fourier Quotient (MFQ)

Proposed by Winsall and Freeman (1993), the MFQ deals very effectively with non-Gaussian BF's by analyzing higher-order normalized moments ($m_n^0 \equiv m_n/m_0$) of the BF. The velocity dispersion is given by m_2^0 and the deviations from purely Gaussian profiles are estimated by means of the *kurtosis*, which, for symmetric functions, is defined as $k \equiv m_4^0/\sigma_x^4$. For a Gaussian BF $k = 3$, for a more peaked BF $k > 3$ and for a less peaked one $k < 3$.

The need for deriving BF moments of higher order than the second makes this method very sensitive to the S/N ratio (which must be ≥ 25).

4.3.2 Direct Fitting Method

Proposed by Rix and White (1992) it consists in parameterizing the galaxy and template spectra into separate components (continuum, absorption line, and noise) and then searching in the parameter space for the combination which minimizes the residuals between galaxy and template. The method does not use the Fourier approach and requires good S/N ratios (≥ 25).

4.3.3 Van der Marel and Franx (1993) method

The observed line profile is expanded as a sum of orthogonal functions in a Gauss–Hermite series (van der Marel and Franx 1993) which offers several advantages:
(i) the zero-th order functions are Gaussians and higher order terms measure deviations from normality;
(ii) the functions carry information on the entire line profile and are less sensitive than higher moments of the velocity to the S/N value in the line–profile wings.

Two parameters are given: h_3, which describes asymmetric deviations, and h_4 to describe the symmetric part.

4.3.4 General remarks

At this point one comment is in order. In spite of all the progress made so far, the measurement of stellar velocity dispersions is still a tricky business and data obtained for the same object in different observing conditions or with different data reduction techniques may led to quite different results. The better agreement is, however, between the FQ and the CC methods, while the FD turns out to provide values systematically lower than the FQ (see also Davoust et al. 1985).

5 Kinematics versus luminosity

In his 1977 paper, Illingworth suggested that low luminosity ellipticals and bulges could be separated from the giant ellipticals in the $(\epsilon, V/\sigma)$ plane. Davies et al. (1983) confirmed that, on average, the velocity anisotropy is correlated to the total luminosity of the system, bright ellipticals having higher anisotropy than faint ones. It needs to be stressed, however, that this correlation is affected by several factors which are impossible to be corrected (such as, for instance, the inclination with respect to the line of sight) and should be used with some caution (cf. Busarello et al. 1992).

Extreme cases, such as NGC 1600 (Jedrzejewski and Schechter 1989), have anisotropy parameter (Sect. 1) $(V/\sigma)^* = 0.013$ and, in the mean, luminous ellipticals have $(V/\sigma)^* \simeq 0.4$. Bender et al. (1989) found that the degree of anisotropy is also correlated with the isophotal shape parameter, boxy galaxies being, on the average, more anisotropic than disky ones.

A more complex trend is observed at the low mass end of the luminosity function of ellipticals ($-17.5 \leq M_B \leq -14$), where two families of objects coexist: compact ellipticals, which seem to be the natural extension of the elliptical sequence, and low surface brightness – also known as diffuse – dwarfs, which have much lower central surface brightness (Kormendy 1985, Djorgovski 1993). Even though firm conclusions are prevented by an endemic dearth of data, induced by the intrinsic faintness of the objects, it seems by now well established that compact dwarf ellipticals are more anisotropic than diffuse ones (Wyse and Jones 1984; Bender and Nieto 1990, Bender et al. 1991). Diffuse dwarf ellipticals have often strange kinematical properties: NGC 205, for instance, has a velocity dispersion decreasing in the inner nuclear regions (Held et al. 1990, Carter and Sadler 1990), a phenomenon which seems to be common also to other dE's (Peterson and Caldwell 1993). Data for dwarf spheroidal galaxies (such as the newly discovered Sextans dwarf) are too scarce to draw any conclusion, and we will ignore them in what follows (see Djorgovski 1993 for an interesting review).

With one known exception, i.e. NGC 4550, which has a non-rotating bulge (Rix et al. 1992), all bulges of spirals and lenticulars observed so far are fast rotators, with an average $(V/\sigma)^* \simeq 0.5$. Even though the unequal behaviour of bulges and ellipticals can be partly understood as an artifact caused by the lack of truly luminous bulges, more likely it reflects an intrinsic and still unexplained difference between bulges and ellipticals. In order to shed light on this matter, detailed studies of the BF's in ellipticals and bulges of comparable luminosity are needed.

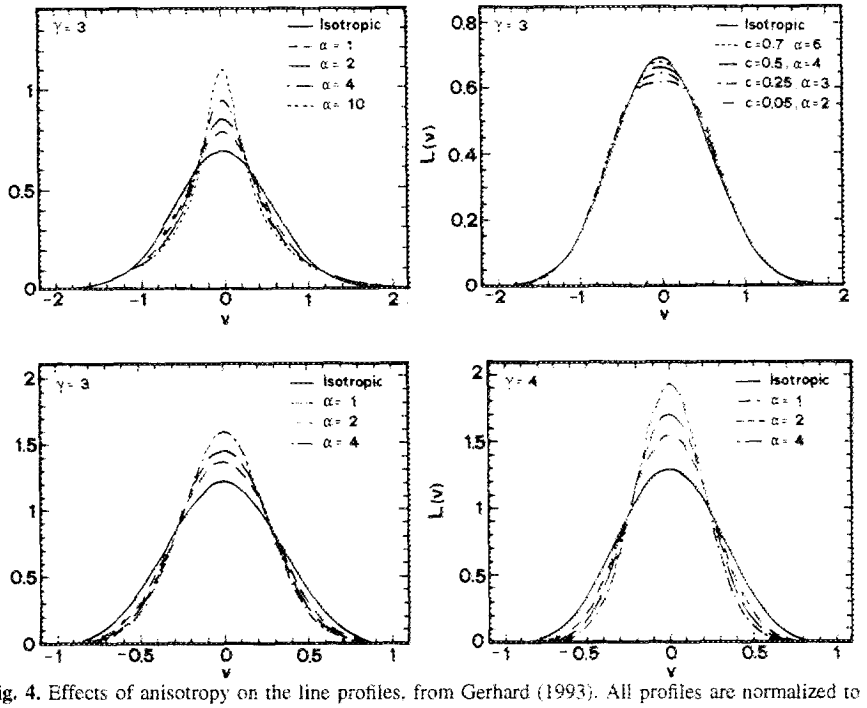

Fig. 4. Effects of anisotropy on the line profiles, from Gerhard (1993). All profiles are normalized to unit integral, and velocities are given in units of the circular velocity. The projected velocity dispersion is the same for all profiles ($\sigma = 0.707$). **a**, **b** Isothermal sphere with $\rho(r) \propto r^{-3}$ in presence of radial **a** and tangential **b** anisotropy. The effects of radial anisotropy are stronger for steeper density profiles: **c** $\rho \propto r^{-3}$, and **d** $\rho \propto r^{-4}$

6 Kinematics as a probe of the intrinsic shape

The intrinsic shape of 'hot' stellar systems has received much attention in the last decade. One reason among many others is that, if the shape of ellipticals is representative of all collisionless systems, it may also provide information on the shape of dark haloes. The anisotropy of the velocity tensor implies that E galaxies need not necessarily be oblate spheroids (Binney 1978); they can be prolate and even triaxial. This conclusion is supported by the discovery that the position angle of the isophotal major axis changes with the radius (see the references given in Sect. 1). In fact, aside from a few interacting galaxies, where the twisting may be induced by tidal torques, and therefore be intrinsic (Kormendy 1977), twisted isophotes find a natural explanation if the isodensity surfaces (i.e. surfaces of constant volume emissivity) are triaxial: the principal axes need not be misaligned, it being sufficient that the axis ratios change with the radius (Stark 1977). Oblate configurations form a subset of the triaxial family; they may display a variable ellipticity but no twisting. However, N-body simulations (Gerhard 1983) have indicated that it is possible to construct objects having intrinsic misalignment of the major axis of the isodensity contours. This fact should be kept in mind and coupled to the consideration that the only manageable models of triaxial systems available so far, i.e. those based on Stackel potentials, do not show any isophotal twisting.

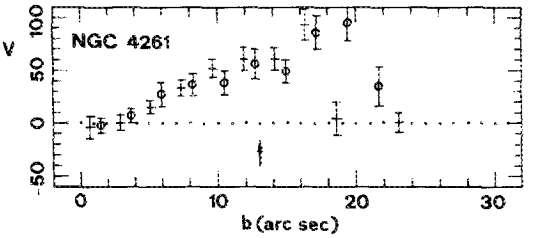

Fig. 5. Rotation along the minor axis for the galaxy NGC4261 (from Wagner et al. 1988)

A variety of statistical tests aimed at establishing the intrinsic shape of ellipticals have been applied to photometric (Binggeli 1980) and kinematical (Binney 1985) data, and to a combinations of the two (Merritt 1982, Capaccioli et al. 1984). For instance, Binney (1978) introduced the $(\epsilon, (\frac{V}{\sigma})^*)$ diagram as a test for triaxiality. This test has been applied many times with discordant results (e.g. Davies et al. (1983), Franx et al. (1989), Busarello et al. 1992), related, among other things, to the impossibility of correcting for the various observational effects and chiefly for the inclinations of the objects with respect to the line of sight.

But the failure of all tests has also deeper roots:
(i) the existence of correlations between the various intrinsic properties (Terlevich et al. 1981);
(ii) the inhomogeneity of the sample (Capaccioli 1987, and references therein);
(iii) the existence of a large spread in central surface brightnesses ($\Delta\mu_B \leq 2$ mag) for the same total luminosity (Capaccioli and Caon 1991; Capaccioli et al. 1992, 1993a).

In a few individual cases, the existence of a dust lane or of a gaseous disk can be used to constrain the orientation and the shape of the objects (e.g. NGC 1052: Davies and Illingworth 1986, Tenjes et al. 1993; NGC 5077: Bertola et al. 1991; NGC 5989, NGC 1947: Tenjes et al. 1993).

6.1 Rotation around the minor axis

The discovery of hot galaxies with appreciable rotation along the projected minor axis (Bertola et al. 1983, Davies and Birkinshaw 1988) was the first clear signature of either triaxiality (Contopoulos 1956, Kondrat'ev and Ozernoy 1979) or occurrence of decoupled/misaligned components (e.g. the case of NGC 3998; Capaccioli 1979, Blackman et al. 1983). In fact, at almost all viewing angles, a triaxial galaxy has an apparent minor axis which does not coincide with the shortest axis of the galaxy. Binney (1985) was first to use the statistics of the rotation along the minor axis to constrain the intrinsic structure. However, he did not take into account that, in a triaxial potential with stationary figure, stellar streaming is allowed along both the major and the minor axis (e.g. Binney and Tremaine 1987). Within each tube orbit all stars can rotate in one direction, or in the opposite one, or in a mixture of the two, thus implying that the angular momentum of the family of orbits may assume any value between zero and the two opposite extremes. Hence the angular momentum of the system may point in any direction within the plane containing the short and the long axis.

Systematic studies of kinematical misalignements have been performed by Wagner et al. (1988), Jedrzejewski and Schechter (1989) and Franx et al. (1991).

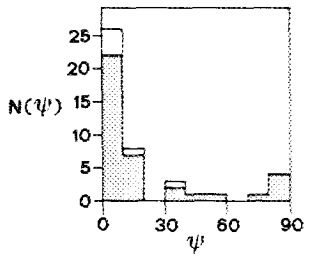

Fig. 6. Histogram of the kinematical misalignments (from Franx et al. 1991). The shaded region refers to galaxies for which the error on ψ is smaller than 25°

Following the same convention adopted by Franx et al. (1989), let ψ be the observed misalignment between the angular momentum and the projected short axis of the galaxy, defined as $\psi = V_{min}/V_{maj}$, where V_{min} and V_{maj} are the rotational velocities along the minor and major axes, respectively. The histogram of ψ for a sample of 22 galaxies is peaked around $\psi = 0$ (Franx et al. 1989), then it declines gradually, with a possible second peak at large values ($\psi > 70°$).

Franx et al. (1991) used the observed distribution of ψ and of the apparent ellipticity ϵ to constrain the three intrinsic (and unknown) parameters: the two axis ratios b/a and c/a, and the intrinsic misalignment ψ_{int}. Let T be the so-called *'triaxiality parameter'*

$$T = (1 - b^2/a^2)/(1 - c^2/a^2) \tag{15}$$

which is = 0 for oblate systems and = 1 for prolate galaxies. Franx et al. (1991) found that, with very good approximation, ψ has a strong dependence on T and ψ_{int}, while ϵ depends mainly on the distribution of c/a. According to Franx et al. (1991), the inversion of the ϵ distribution shows a peak near $c/a = 0.6 \sim 0.7$, and is almost zero for round galaxies. Franx et al. (1991) also find that $\langle T \rangle \leq 0.4$ and $\langle \psi_{int} \rangle \leq 20°$. Small kinematical twists can be explained in terms of projection effects alone, but large misalignements (such as those observed in NGC 4365 and NGC 4406; Bender 1988b, Wagner et al. 1988) require large intrinsic misalignments of the angular momentum, which are possible only in a triaxial potential. The generalization of these results, however, should be reviewed in the light of the conclusion that minor axis rotation has been found, so far, only in boxy ellipticals.

7 Dynamical subcomponents

In what follows we will adopt the widespread attitude of considering stellar systems as the superposition of different subcomponents only mildly interacting with each other. This approach is not fully justified by observational evidence and can very often lead to misleading interpretations (see Balcells 1992). However, it seems so far the only way to order the available wealth of data (cf. Djorgovski 1994). Each subsystem is characterized by its density distribution, dynamics, and composition (stars, dark matter, etc.), and by the geometrical (location inside the galaxy, intrinsic shape, etc.) and physical parameters of the various components.

7.1 Faint stellar disks

The search for faint stellar disks hidden within ellipticals was stimulated by the substantial continuity of properties existing between E's and S0's for vanishingly small disk-to-bulge ratios (Simien and de Vaucouleurs 1986, Capaccioli 1987, Capaccioli et al. 1990b, Capaccioli and Longo 1990, van den Bergh 1990, Michard and Marchal 1993). Earlier investigations of the luminosity profiles (where disks appear as weak signatures: Capaccioli and de Vaucouleurs 1983, Lauer 1985, Carter 1987) and of the geometrical properties (Michard 1984) lead to conflicting results. A more powerful tool is the isophotal shape analysis already mentioned in Sect. 1.

The most straightforward explanation of disky ellipticals (Capaccioli 1987; Carter 1987) is that *'pointed'* isophotes originate from a weak stellar disk embedded into a much larger spheroid . It needs to be stressed, however, that alternative explanations have been proposed (cf. Stiavelli et al. 1991).

Capaccioli (1989), Capaccioli et al. (1990b), and Rix and White (1990) have shown that even relatively strong stellar disks (bulge-to-disk ratio $B/D \simeq 5$) can escape detection unless their orientation is close to edge-on. Therefore, many ellipticals might contain disks which are not detected by photometric means, but which nonetheless affect with their presence the rotational velocity and the central velocity dispersion, which tend to be overestimated and underestimated, respectively. Capaccioli et al. (1990b, 1992) find that most, if not all, low/intermediate luminosity ellipticals contain disks, the only objects which are very likely to be devoid of disks being some luminous ellipticals and the brightest cluster members.

The presence of a disk produces an asymmetry in the high velocity wing of the BF, which lowers the 'true' value of σ_0 by as much as 20%, thus leading also to overestimating of the degree of anisotropy of the object (Fig. 7). Good examples are NGC 3585 (Bender et al. 1993) and NGC 2974 (Cinzano and van der Marel 1993) where, once the disk contribution has been removed, the spheroids turn out to be pressure supported. The accuracy of these results is confirmed by the fact that in the above cases, the B/D ratios obtained from the kinematical data and from the decomposition of the light profile agree, on average, within 5%.

One striking feature of many disky ellipticals is that there seems to be at work the same sort of *'conspiracy'* observed in lenticulars and spirals: the rotational velocity of the outer bulge is equal to the mean rotational velocity in the inner parts, where the dominant contribution comes from the disk. Several exceptions to this behaviour are however known.

One of the most conspicuous example of how bulge and disk can combine to produce peculiar kinematical behaviours is that of the elliptical NGC 3585, a galaxy with a high rotational velocity (Bender et al. 1993). Its velocity dispersion decreases outwards in the inner 12 arc seconds to rise again in the outer regions; the rotation curve shows instead the opposite trend, raising in the inner 12 arcsec and then dropping outwards (Fig. 7). The BF is clearly asymmetric and a simple double-Gaussian fit allows to separate the contribution of the disk and bulge. The disk – which is detected also by photometric means – is conspicuous and contributes up to 80% of the light in the intermediate regions. Once the disk contribution has been removed, the bulge turns out to rotate very slowly and to have a high degree of anisotropy ($(V/\sigma)^* \simeq 0.25$).

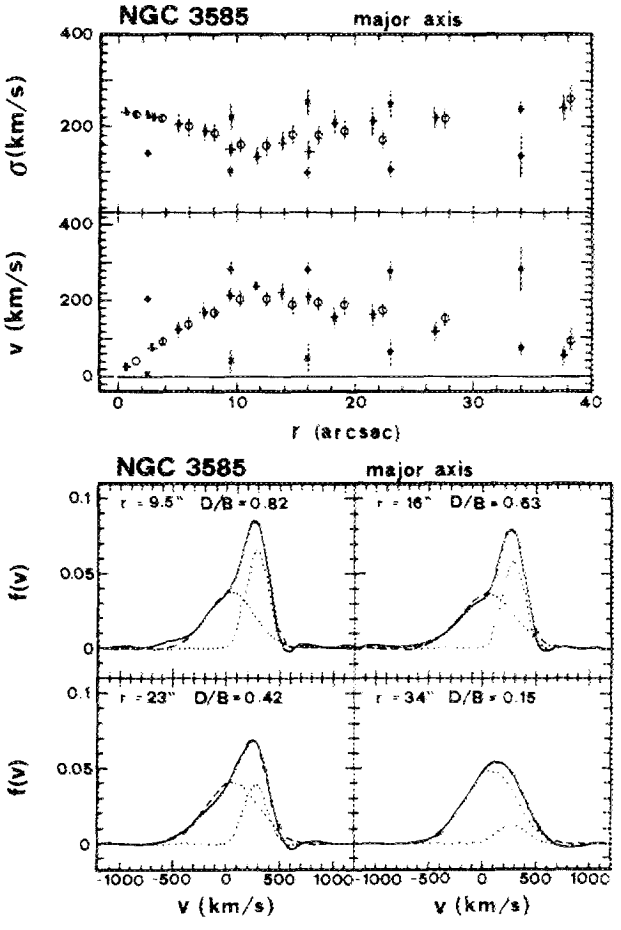

Fig. 7. Taken from Bender et al. (1993). Upper panel: rotation curve and velocity dispersion profile along the major axis for the disky elliptical NGC 3585. Larger symbols correspond to the profiles which would be derived by using standard single-Gaussian fitting techniques (e.g. FCM). Smaller symbols are obtained by using a two-Gaussian fitting algorithm and give the rotation curve and the velocity dispersion profiles of the bulge (*x-shaped*) only and of the disk (*crosses*) only. Lower panel: fit of the BF at four different positions obtained with the two-Gaussians model

7.2 *Kinematically decoupled cores (KDC's)*

Related to the previous topic is the nature of the kinematically decoupled subcomponents observed in the central regions of some galaxies. In the case of bulges (Dressler 1984, Kormendy 1988b) and of a few ellipticals (e.g. NGC 5813, Efsthatiou et al. 1982), the peculiarity consists in a sharp increase of the rotational velocity in the inner parts (see also Capaccioli 1979). In other cases the angular momenta of the inner and of the outer regions appear misaligned (e.g. IC 1459; Franx and Illingworth 1988).

Far from being rare, KDC galaxies comprise a large fraction of all ellipticals. Owing to selection effects, the estimated frequency, $\geq 20-25\%$ (Franx et al. 1989), must be regarded as a lower limit. In fact, firm statistical conclusions are hampered by:

(i) the widespread habit of taking spectra along the major and minor axes only (Wagner 1990), which biases the findings towards large effects only and yet prevents the measurement of the exact amount of the misalignments;

(ii) the usually low spatial resolution of most data available in the literature;

(iii) observational bias associated with the fast decrease in surface brightness (Franx 1990), which seems to favor the detection of KDC's of small apparent sizes (typically $\sim 5''$ to $10''$; see the list in Bender's, 1990a).

The large fraction of E's with kinematically decoupled cores implies that, whatever the mechanism leading to the formation of KDC's is – either genetic or evolutionary –, it must be a common one.

Current interpretations of KDC phenomenology can be divided into two groups: the 'core–within–a–core' (hereafter CWC), which assumes the decoupled component to be spheroidal in shape, and the 'bulge/disk' which instead imagines it to be a weak stellar disk. Kinematically decoupled CWC's are expected to form from the merger of a small-sized high-density galaxy with a large-sized low-density one (Kormendy 1984b, Balcells and Quinn 1990), the counter-rotation being induced by the tranfer of orbital angular momentum. The 'bulge/disk' interpretation encompasses instead a large variety of possibilities: tidal disruption of a small gas-poor satellite galaxy, the debris of which sinks into the potential well forming a disk shaped remnant (Illingworth and Franx 1989), the merger of two spirals (see for instance the case of NGC 520; Stanford and Balcells 1990), and the accretion of a small gas-rich galaxy into a normal elliptical (NGC 3656; Balcells and Stanford 1990). In the last two cases the accreted gas would settle onto one of the principal planes of the remnant galaxy (see Sect. 7.3), eventually leading to stellar formation and to a kinematically decoupled stellar disk (for a thorough discussion see Balcells 1992).

Most of the observed properties of KDC's can be explained either by the CWC or by the 'bulge/disk' models.

(i) In a fairly large sample of galaxies (but not all; see, for instance, NGC 2663 in Carollo and Danziger's, 1993), a sharp increase in metallicity is observed at the transition between the kinematically decoupled region and the main body of the galaxy (Bender and Surma 1992). This trend is predicted both by the CWC models – on average low luminosity ellipticals are bluer (Sandage and Visvanathan 1978) –, and by the 'bulge/disk' models – stars formed from the remnant of a gas-rich galaxy are expected to have higher metallicity.

(ii) In the few well studied cases (e.g. IC 1459 and NGC 5322; Rix and White 1992), the line profile is strongly asymmetric, with the asymmetry changing sign while crossing the nucleus. In the case of IC 1459, the anisotropy parameter of the KDC

has a quite high value ($\simeq 2$). These facts can be easily understood in both the CWC (see discussion in Balcells 1992) and the 'bulge/disk' scenarios (Franx and Illingworth 1991).
(iii) The existence of a very disturbed kinematics in the KDC of NGC 7626 can be explained only by a recent accretion event (age $< 10^8$ yr; Balcells and Carter 1993). The absence of any starburst signature in the spectrum is supportive of the CWC scenario.
(iv) The CWC hypothesis seems favored by the fact that most, if not all, ellipticals harboring KDC's have 'boxy' isophotes (Balcells 1992).
(v) In spite of several systematic searches, so far no misaligned KDC's have been observed in bulges of spirals (Fisher et al. 1993) and lenticulars (Rubin et al. 1992, Franx 1993): a result which is compatible with the 'bulge/disk' model, due to the fact that pre-existing gas favors co-rotation of the accreted material through shock heating. The only possible exception, NGC 4594 (Kormendy and Westphal 1989, Hes and Peletier 1992), has however an abnormally large bulge, comparable in size to a giant elliptical.

A possible alternative explanation of KDC's is that the figure rotation velocity is backward with respect to the streaming velocity of stars. This, however, is contradicted by the unlikeliness of counter-streaming (Vietri 1986) and by the impossibility of explaining kinematically decoupled systems other than those with antiparallel spins.

One fact to be always kept in mind is that the two-body relaxation time is so large that the expected lifetimes of KDC's are longer than several Hubble times. Therefore, KDC's might just be a consequence of the generic formation process of ellipticals (Barnes and Efstathiou 1987). It seems therefore realistic and safe to conclude that, at the present state of knowledge, the KDC's phenomenology is likely to be the result of several different processes.

7.3 Kinematics of gaseous disks and dust lanes

Further evidence in support of the accretion of gas from the environment comes from emission line measurements (both in the optical and in the radio ranges). In fact, despite early beliefs, a large fraction ($30 \sim 40\%$) of early-type galaxies contains non-negligible amounts of dust (Hawarden et al. 1981, Sadler and Gerhard 1985, Kormendy and Stauffer 1987). A significant fraction ($\geq 10\%$) contains also gas both in the atomic ($10^4 \sim 10^9\ M_\odot$) and in the molecular ($10^5 \sim 10^8\ M_\odot$) form. Warm, ionized gas (Demoulin–Ulrich et al. 1984; Trinchieri and Di Serego 1991; Macchetto and Sparks 1992) and hot X–ray gas have also been detected (see Sect. 8.4).

The various phases of the interstellar medium are distributed differently: dust is usually organized in dust lanes or patches (Bertola 1987), cold atomic gas is mainly distributed in rings or disks (van Gorkom 1992), and molecular gas is centrally peaked (Lees 1991, Quillen et al. 1991). Warm ionized gas exhibits a complex morphology (Baum et al. 1989). The exact fraction of early-type galaxies containing gaseous components is difficult to evaluate due to selection effects which favor the detection of disks having large inclinations with respect to the line of sight (Amico et al. 1993). It is however larger than 20%.

So far, the most useful dynamical implications come from the atomic gas. Gaseous disks are often highly inclined with respect to the principal plane of the galaxy and have specific angular momenta much larger than for the stellar component (e.g. NGC 7097, Caldwell et al. 1986). In a few cases (e.g. IC 2006, Schweizer et al. 1989,

or NGC 2768, NGC 4379, and IC 4889, Bertola et al. 1992) gas is even counter-rotating with respect to the stars. The decoupling of the cold gaseous component from the stellar one is also confirmed by the form of the distribution function $n\left(M_{HI}/L_B\right)$ for the relative HI content (Knapp et al. 1978), which is completely different from that observed in later galaxy types.

All these arguments support the idea that in early-type galaxies gas has been accreted from the environment. In some cases (e.g. NGC 1052; van Gorkom et al. 1986, Davies and Illingworth 1986), despite the patchy and chaotic distribution, the velocity field of the ionized, atomic, and molecular gas turns out to be quite regular, thus suggesting that the gas has had at least the time to settle into an equilibrium plane.

Theoretical studies of the settling process show that small amounts of gas or dust infalling into a spheroidal axisymmetric potential can reach a stable configuration only in the equatorial plane, while in triaxial, non-rotating potentials, there are two possible equilibrium planes perpendicular to the shortest and the longest axes (Schwarzschild 1979, Steiman–Cameron and Durisen 1982, Merritt and de Zeeuw 1983, Steiman–Cameron et al. 1992), known as the equatorial and meridian planes, respectively. If the accreted material is massive enough, it can settle in a stable warped configuration away from the principal planes (Sparke 1986, Arnaboldi and Sparke 1994). The angular momentum of the accreted gas can be either perpendicular, or parallel, or even anti-parallel to the stellar component. Thus the statistics of counter-rotating gas should be different in gas rich and gas poor systems, although the available data are insufficient to draw firm conclusions.

The time scale for the accreted gas to settle down onto one of the principal planes can be a large fraction of the Hubble time (Steiman–Cameron and Durisen 1982, 1988). This is supportive of the suggestion by Schweizer et al. (1989) that, at least in some cases, the gas can be a leftover of the merging process from which the elliptical galaxy was formed.

In the case of lenticulars, the line–emission is usually confined to the bulge-dominated regions. Bertola et al. (1992) find that $\sim 20\%$ of S0's host gaseous components which are decoupled from the stellar ones (they also give an up-to-date list of objects). In a few extreme cases (e.g. NGC 2768 and 4739, and IC 4889) the spins of the two components are anti-parallel.

7.4 Narrow polar rings

Narrow polar rings are annuli almost perpendicular to the principal plane of the host galaxy, most often a lenticular, and are confined inside its optical boundaries. Their nature is not yet fully understood. They are usually interpreted as transient phenomena produced by recent accretion (Schweizer et al. 1983), even though the kinematics of AM 2020-504 is better reproduced by a stable warped structure (Arnaboldi et al. 1993a). Recent accretion is supported by the detection of a KDC component and of a strong UV continuum (Arnaboldi et al. 1993a, 1993b), and by the discovery of CO emission (Combes et al. 1992, Arnaboldi et al. 1993c).

Most polar rings are remarkably flat and are often tilted with respect to the polar axis by as much as 35° (Whitmore 1991). This is not an obvious property for a structure embedded in the axisymmetric potential of lenticular galaxies, where the quadrupole component of the field would induce precessional torques capable of destroying the flatness in much less than an Hubble time (Schechter et al. 1984).

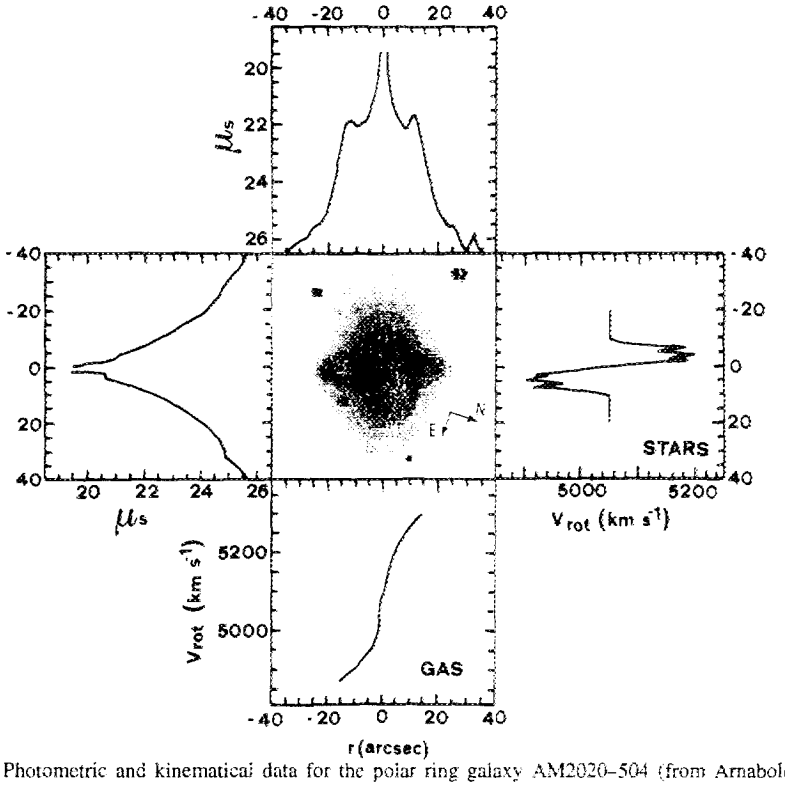

Fig. 8. Photometric and kinematical data for the polar ring galaxy AM2020–504 (from Arnaboldi et al. 1993a)

Two possible explanations have been proposed: either polar rings are recent transient structures, or there are some physical mechanisms which stabilize them against tidal disruption. Two mechanisms have been proposed:
(i) the presence of a static triaxial potential with two principal planes, which would explain an inclination $\Delta\theta \simeq 90°$ between the ring and the stellar component, or a tumbling triaxial potential, when $\Delta\theta < 90°$ (van Albada et al. 1982; Tohline and Durisen 1982);
(ii) self gravitating polar rings in a flattened potential, where the mutual attraction of the particles can stabilize the ring and force it to precess as a unit (Sparke 1986, Arnaboldi and Sparke 1994).

One additional puzzling feature of polar rings, i.e. the existence of the central hole, has been explained in terms of shock waves arising when the supersonic gas forming the polar disk interacts with the gas in the galactic disk (Wakamatsu 1993).

7.5 Central black holes

The kinematical signature of a massive black hole in the nuclear region of a galaxy is a very steep gradient in both v and σ (Carter and Jenkins 1993). The implied measurements require very high spatial resolution and are therefore possible only for the nearest objects (see Kormendy 1987, and references therein). Besides the

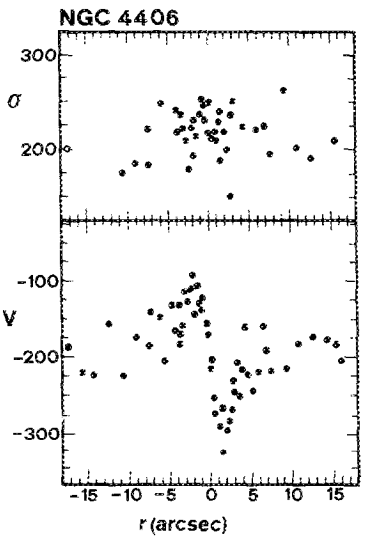

Fig. 9. The velocity dispersion profile (upper panel) and rotation curve (lower panel) of NGC 4406 at P.A. = 120° (from Carter and Jenkins 1993). Velocity dispersion has a peak in the inner 2". The core of this galaxy rotates along the photometric minor axis while the outer parts rotate around the major axis. This galaxy has long been a candidate to host a nuclear black hole. Carter and Jenkins (1993) however, showed that the data can be explained also by a relatively bright stellar disk

classical example of M87 (Sargent et al. 1978, Young et al. 1978), galaxies which have been from time to time candidates to host a nuclear black hole are, for instance, M 31 (Dressler and Richstone 1988, Kormendy 1988a, Carter and Jenkins 1993), M32 (Dressler and Richstone 1988; Richstone et al. 1990; Tonry 1984, 1987), NGC 4594 (Jarvis and Dubath 1988, Kormendy 1988b), NGC 3115 (Kormendy 1987, Kormendy and Richstone 1992), NGC 5813 and NGC 4406 (Carter and Jenkins 1993; see also Fig. 9). The interpretation of the kinematical observables, however, is ambiguous due to projection effects as well as to finite spectral and spatial resolution (e.g. Carter and Jenkins 1993).

It needs also be stressed that steep kinematical gradients do not necessarily imply a supermassive black hole: a moderate amount of anisotropy (Duncan and Wheeler 1980, Dressler and Richstone 1990), or a small nuclear bar viewed down its major axis (Gerhard 1989), can explain the observations while maintaining a constant mass-to-light ratio.

But even in the case of truly high values of (M/L), a likely alternative is a dense cluster that, for instance, can be formed during a core collapse phase (Dressler and Richstone 1988; Michard and Nieto 1991). This hypothesis however, seems very unlikely at least for M 31, where recent HST data have shown the existence of a second cusp in the light distribution at few arc seconds from the photometric nucleus of the galaxy (Tod Lauer, HST News).

Several authors (Norman et al. 1985, Gerhard 1987) investigated the effects of a massive black hole on a triaxial potential, finding that scattering processes would destroy triaxiality in the inner regions. Such an effect seems to be present in the data of Franx et al. (1989), but the sample is too small to draw definite conclusions.

8 Outer kinematics

The outer (i.e. $r > r_e$) kinematics allows us to gauge the halo mass distribution and to seek for the formation history. For instance, Hernquist (1993) carried out numerical simulations showing that in a merger between two identical galaxies, the inner regions are expected to rotate much slower than the outer ones. Also, even though the existence of dark matter seems to be well established at all scales, from dwarf galaxies to the richest clusters, its presence in early-type galaxies is still a matter of debate. This unfortunate situation is due to several concurrent factors. The cold gas content is limited (see van Gorkom 1992, and references therein) and HI usually is not measured out to large galactocentric distances; the cold and warm gas are usually of recent accretion (see Sect. 7) and may have not yet settled into equilibrium configurations. The interpretation of the X-ray emission from the hot gas coronae is too much dependent on the model parameters to allow reliable conclusions (Sect. 8.4). The only possible kinematical tracers are therefore either the rotation curves derived from stellar absorption features, or the overall kinematical properties of bright tracers of the potential – such as globular clusters or planetary nebulae – which can be detected out to large distances and form a dynamically homogeneous population.

8.1 Extended rotation curves

So far only a few stellar rotation curves extending beyond $1.5r_e$ have been measured by adopting special observing (Cappellaro et al. 1989; Capaccioli et al. 1993a; Bertola et al. 1992; Amico et al. 1993) and data reduction (Richter et al. 1992) strategies. The observational efforts have concentrated on both S0's and normal ellipticals.

The case of the close to edge-on lenticular NGC 3115 (Capaccioli et al. 1993a) shows a rotation curve which increases steeply in the inner regions to reach 260 km $s^{-1}$and then remains flat out to the last measured point ($\simeq 2r_e$). The velocity dispersion instead decreases smoothly in the inner regions to stabilize at about 100 km s^{-1}in the outer ones. A simple model predicts an increase of (M/L) of a factor ~ 2 from the inner to the outer regions. Similar results have been obtained for other edge-on lenticulars by Cappellaro et al. (1990).

The few data so far available for ellipticals show that most rotation curves remain flat even at large galactocentric distances; the velocity dispersion profiles may have instead very different trends. In most cases, velocity dispersions decrease outwards but for a few, noticeable exceptions (e.g. NGC 5813, Efsthatiou et al. 1982, Davies and Birkinshaw 1988; NGC 4472, NGC 7714, and IC 4296, Saglia et al. 1993a), they remain flat well beyond the effective radius.

Increasing velocity dispersions at large radii are common among cD's (Dressler 1979, Carter et al. 1981, 1985) and are possibly detected (but the data are doubtful) in the normal, non-interacting elliptical NGC 7144 (Saglia et al. 1993a). As clearly stated by Saglia et al. (1993a), the interpretation of these results is ambiguous; the data can be fitted either by assuming a two component self-consistent spherical and non-rotating model, which leads to a (M/L) increasing outward, or by assuming a constant value of the mass–to–light ratio and then looking for a physical justification of the phase space structure. We shall remark, however, that the values of (M/L) obtained in the second case are too high to be realistic in the absence of dark matter.

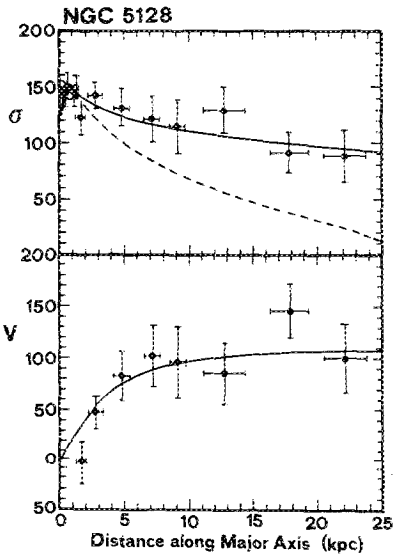

Fig. 10. Rotation curve and velocity dispersion profile of NGC 5128 as obtained from the planetary nebulae. The solid line gives the kinematics predicted by a simple two components (dark halo + luminous matter) model, while the dashed line gives the kinematics predicted by a selfconsistent isotropic model which fits well the data in the inner regions (from Hui et al. 1993)

All attempts to disentangle these two factors on the basis of theoretical assumptions on the velocity distribution function are very much model dependent. The techniques mentioned so far are bound to become obsolete due to the line profile asymmetries method which allows the direct measurement of the velocity anisotropy.

However the relatively high S/N ratio required by the various line profile asymmetry methods makes it almost impossible to obtain reliable data beyond $2.0r_e$ (Amico et al. 1993) and, at larger galactocentric distances, other types of kinematical tracers are required.

8.2 Outer kinematical tracers. The case of NGC 5128.

The use of test–particles such as globular clusters (GC) and/or planetary nebulae (PN) to probe the halo potential of early-type galaxies is still in its pioneering stage, and many contradicting results are spread in the literature (compare for instance, Ciardullo et al. 1993, to Merritt and Tremblay 1993).

Globular clusters are difficult to identify beyond 30 Mpc and, with the current technology, their radial velocities cannot be measured at distances greater than $\sim 10 \sim 15$ Mpc. In spite of their intrinsic faintness, planetary nebulae appear to be better tracers: they can be easily identified by means of interference filters centered on the 5007 Å [OIII] emission line, and their radial velocities can be derived from emission rather than absorption features (Ciardullo et al. 1993).

A good example of how both GC's and PN's can be used to constrain the outer kinematics is provided by the well known peculiar elliptical NGC 5128 (but see also the case of NGC 3379, Ciardullo et al. 1993), where radial velocities have been obtained for 62 GC's (Sharples 1988; Harris et al. 1988) and for 433 PN's (Fig. 10).

The kinematics in the inner regions of NGC 5128 has been obtained for both the stellar component (Wilkinson et al. 1986) and for the $H\alpha$ (Bland et al. 1987, Nicholson et al. 1992) and the HI gaseous emissions (van Gorkom et al. 1990). The generalization of the results obtained for this very peculiar galaxy is not trivial, but some interesting conclusions can be reached.

The PN–based velocity field extends out to $4r_e$ (i.e. $\sim 20 \sim 25$ kpc) along the photometric major axis. It presents a clear misalignement ($\sim 39°$) of the kinematical rotation axis with respect to the photometric minor axis, thus implying that at least in the outer halo, the potential is strongly triaxial. We note, however, that the rotation axis and the direction of maximum rotational velocity are not orthogonal. The rotational velocity reaches a maximum at about 7 kpc and remains flat out to ~ 20 kpc. The velocity dispersion is ~ 143 km s^{-1} at about 2.8 kpc, and declines to ~ 90 km s^{-1} at ~ 20 kpc (Hui et al. 1993).

The agreement between the PN data and the inner kinematics is quite good. On the assumption that also the outer PN's have reached the equilibrium, the data point toward a mass-to-light ratio strongly increasing outwards and to a decoupling between the inner regions, which are more likely to be isotropic, and the outer ones, which are strongly triaxial.

The kinematics of the GC's system, instead, seems to be decoupled from that of both the stellar component and the PN's. It must be noted, however, that due to the large mass difference, the collision rate between globular clusters and stars within a galaxy can be relatively large (Pesce et al. 1992). This implies that the globular cluster halo can be a partly collisional system and that some secular evolution may result from the coupling of these two components (Bertin and Stiavelli 1993).

We stress that the interpretation of the results obtained by means of test-particles such as PN's or GC's, is strongly model-dependent. Merritt and Tremblay (1993) have studied the kinematics of the outer halo of M 87 using the radial velocities obtained for a sample of 43 GC's by Mould et al. (1990), reaching the following conclusions:
(i) assuming isotropy, the dynamics of the globular cluster systems around M 87 can be constrained out to $\simeq 50$ kpc, and the total mass derived within this radius is 60×10^{12} M$_\odot$, in agreement with the X–ray halo estimates. The dark matter density in the outer halo decreases as $\rho_{dm} \propto r^{-1.8}$. The error on the exponent is however quite large. In order to reduce it to ± 0.5 we should measure the radial velocities of ~ 200 GC's;
(ii) to relax the hypothesis of isotropy would require a number of radial velocities at least one order of magnitude larger (i.e. $\sim 10^3$).

8.3 Wide annulus polar rings (WAPR)

This class of object has been formally introduced by Whitmore et al. (1990), even though specific cases were known to exist long before (e.g. A0136-801, NGC 4650A; Schweizer et al. 1983, Whitmore et al. 1987). They are S0 galaxies circled by a wide annulus of dust, gas, and stars, aligned with the galaxy minor axis and extending out to 4 times the galaxy optical size. Schweizer (1983) and Sackett and Sparke (1990) have shown that WAPR's can be used to map the tri-dimensional shape of the outer halo, obtaining a rather flat distribution (E3÷E7) for the case of NGC 4650A.

8.4 X–ray haloes

X–ray halos have been thought for a long time to be valuable probes of the outer potential well (Forman et al. 1985; Thomas 1986, Lowenstein 1992; see also the extensive review by Sarazin 1986). However, Bertin (1993) has recently shown that complexities intrinsic to the physics of the hot coronae make it impossible to derive the underlying potential well. In particular, in the standard steady–state cooling flow model, the predicted emission and temperature profiles of the hot gas are very model dependent, and even large variations in the expected overall $\langle M/L \rangle$ ratio do not produce appreciable effects.

This situation cannot be changed by increasing the resolution of the X–ray data due to the difficulties in disentangling the relative contributions to the X–ray flux coming from discrete sources and the surrounding cluster.

9 Global properties

Global properties of ellipticals are not distributed at random. This statement has an immediate theoretical justification in the fact that any dynamical model of a collisionless stellar system can be scaled in mass, radius, and central velocity dispersion, with these three parameters constrained by the Virial Theorem (Binney and Tremaine 1987).

9.1 The Virial Theorem

The following equation must hold for any galaxy bound by newtonian gravity

$$\frac{GM}{\langle R \rangle} = k_E \frac{\langle V^2 \rangle}{2}, \tag{16}$$

where G is the gravitational constant, M the total galaxy mass, R a radius such that the left-hand side of Eq. 16 is the potential energy, k_E the virialization constant ($k_E > 1$ for bound systems and = 2 for virialization), and $\langle V^2 \rangle / 2$ the mean kinetic energy per unit mass. In order to enable us to use Eq. 16, $\langle R \rangle$, $\langle V^2 \rangle$, and M, must be replaced with *observables*. By adopting the same notation of Djorgovski and Santiago (1993), we introduce:
(1) some kind of non-isophotal radius, e.g. from a light–profile model fit with an isothermal (King 1966) or with a $r^{1/4}$ (de Vaucouleurs 1948) law

$$R = k_R \langle R \rangle \tag{17}$$

The constant k_R reflects the density structure of the galaxy;
(2) some sort of velocity scale, e.g. the central velocity dispersion σ_c for ellipticals (it would be the maximum rotational velocity V_{max} for spirals)

$$V^2 = k_V \langle V^2 \rangle \tag{18}$$

Here k_V reflects the kinematical structure of the galaxy;
(3) an average surface brightness I such that

$$L = M/\langle M/L \rangle = k_L I R^2 / \langle M/L \rangle \tag{19}$$

where $\langle M/L \rangle$ is the global mass-to-light ratio, k_L reflects the luminosity structure of the galaxy, in general different from the density structure.

Obviously k_R, k_V, and k_L, depend on the adopted definitions, while k_E does not: it is an *intrinsic quality* of the galaxy, which is set by the overall energy dissipation during galaxy formation.

By substituting the 'observables' as defined by Eqs. 17, 18 and 19, into Eq. 16, and by defining the combined structural parameters:

$$K_1 = k_E/(2Gk_Rk_Lk_V) \tag{20}$$

$$K_2 = k_E^2/(4G^2k_R^2k_Lk_V^2) \tag{21}$$

we obtain two relations:

$$R = K_1V^2I^{-1}\langle M/L \rangle^{-1} \tag{22}$$

$$L = K_2V^4I^{-1}\langle M/L \rangle^{-2} \tag{23}$$

which can be used as distance indicators. The quantities R and L are *distance-dependent*, while those on the right-hand side are not.

By assuming that $K_{RS}\langle M/L \rangle^{-1}$ is a power–law function of R, V, or I alone, Eq. 22 translates into the well known *fundamental plane* relation $R \propto V^{1.4}I^{-0.9}$ (Djorgovski and Davis 1987), which is equivalent to the $D_n \propto \sigma$ relation proposed by the *seven samurai* (Dressler et al. 1987).

Similarly, Eq. 23 may read as the Faber-Jackson relation $L \propto V^{\alpha}$, with $\alpha \simeq 4$, if $K_2I^{-1}\langle M/L \rangle^{-2}$ is a power–law function of L or V.

Besides being useful, the fact that Eqs. 22 and 23 work well for early-type galaxies is extraordinarily important since it indicates that the structural conditions implied by Eqs. 17, 18 and 19, hold. In turn, these conditions set constraints on the formation processes and subsequent evolution of early-type galaxies.

9.2 More on global properties

Since the early sixties it has been known that the luminosity L correlates with the linear effective radius R_e (Fish 1964), central velocity dispersion (Faber and Jackson 1976), mean effective surface brightness (Binggeli et al. 1984), colors (Sandage 1972), and average metallicity (Terlevich et al. 1981). The rather large scatter of these correlations led to the discovery that, in the 3-D space $S(\sigma_0, \mu_e, R_e)$, all 'hot' stellar systems (including bulges) are confined within a quite narrow region known as 'fundamental plane' (hereafter FP; Djorgovski and Davis 1987, Dressler et al. 1987). The FP is not uniformly populated, but galaxies are located in a sort of *'fundamental ribbon'* (Guzman et al. 1993). Roughly speaking, the existence of the FP means that the total mass (σ_0), the mean density (μ_e), and the scale length (R_e) of 'hot' galaxies are tightly correlated. According to Djorgovski (1994):

$$\log R_e = 1.49\left(\log \sigma + 0.23\langle \mu \rangle_e\right) - 6.6 \tag{24}$$

The surprisingly low dimensionality of the FP implies that the processes involved in the formation of 'hot' stellar systems are not too numerous, the main driving parameter being very likely the total mass.

The fact that the FP does not depend on details of the shape of the light distribution such as, for instance, ellipticity, isophotal twist rate, isophotal shape parameter, etc.,

means that these details must result from some stochastic processes which operate separately from the main formation mechanisms responsible for the global parameters.

While the existence of the FP cannot be doubted, its slope and zero point are still controversial (e.g. Djorgovski and Santiago 1993). There is a weak but undeniable dependence on the degree of anisotropy: more rotationally supported galaxies are far away from virialized configurations, and show a stronger dependence of $\langle M/L \rangle$ on the mass (see also van der Marel 1991, and Saglia et al. 1993b). Even though in principle ellipticals can span a large variety of dynamical models, in practice the thinness of the FP implies that this is not the case and that only a small range of velocity anisotropies is covered.

The behaviour of the FP at the low luminosity end can shed some light on the properties of diffuse dwarfs. Even though data available in literature are mostly restricted to diffuse E's with bright nuclei (Peterson and Caldwell 1993), it is well established, that dwarf ellipticals are not located on the FP (Fig. 11; Djorgovski 1993) but rather form a one-parameter family (Peterson and Caldwell 1993).

One more fact which so far has not found any satisfactory explanation is the segregation discovered by Capaccioli et al. (1992, 1993b) in the plane defined by the effective parameters $(\mu_e, \log R_e)$ (where R_e is the linear effective radius expressed in kpc). In this plane, ellipticals separate into two families: a *'bright'* one, having $M_B \leq -19.3$, and an *'ordinary'* family. Bright ellipticals follow an Hamabe–Kormendy (1987) relation (μ_e depends linearly on $\log R_e$ only), while ordinary E's are distributed in a wide strip (the total luminosity depends on both μ_e and R_e), with a sharp cutoff at $R_e \leq 3$ kpc.

As for the luminosity profiles, the wide applicability of the $r^{1/4}$ law should not be confused with universality. For most luminosity profiles, in fact, the fit is performed over too narrow a radial range, and systematic deviations from an ideal $r^{1/4}$ law may be easily overlooked. Caon et al. (1993) have recently shown that if photometric profiles extend over a large enough range in surface brightness, the generalized de Vaucouleurs formula (or Sersic law):

$$\mu(r) = \mu_e + c_n \left[\left(\frac{r}{r_e} \right)^{1/n} - 1 \right] \tag{25}$$

provides a much better fit to the data. This is not just an artifact of the one additional fitting parameter, as is shown by the clear correlation existing between the exponent n and the effective radius or the absolute magnitude.

9.3 Masses and mass-to-light ratios

Many different approaches have been attempted to derive the total masses and the average mass-to-light ratios of spheroidal systems from kinematical and photometric data. Most methods are based on the Virial Theorem (Faber and Gallagher 1979, Bacon et al. 1985). Virial masses have also been derived from X–ray haloes (Forman et al. 1985). Another technique is based on the hydrodynamical equations (Binney and Tremaine 1987).

The most effective methods, however, are the self-consistent ones, where photometry and kinematics are used to constrain the degrees of freedom of detailed models: Katz and Richstone (1985), Bertin et al. (1988), Bettoni et al. (1991), Capaccioli et al. (1993a). Van der Marel et al. (1990) constructed axisymmetric dynamical models

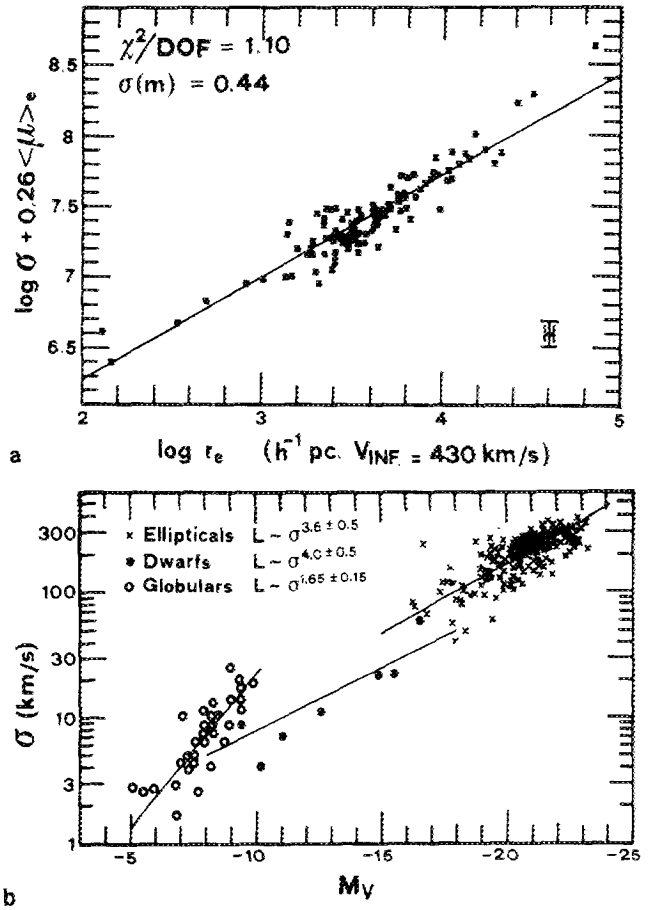

Fig. 11. a One of the many representations of the FP (Djorgovski and Davis 1987); the view is edge-on and the residual scatter is fully accounted for by the observational errors. b Relations between the absolute visual magnitude M_V and σ for a sample of GC's, diffuse dwarf E's and normal E's (from Djorgovski 1993)

for galaxies having photometric and kinematical data along both the major and the minor axes.

All these methods provide estimates for M/L comprised in the range $5 \sim 15$ in a large range of masses: from dwarfs (Peterson and Caldwell 1993) to giants (Saglia et al. 1992). These values are higher than those typical of stellar disks or globular clusters but cannot be considered as a proof in favour of the existence of large amounts of dark matter. Both disks and GCs, in fact, are expected to have relatively low M/L due to the presence of young stars or to the evaporation of neutron stars (Hut et al. 1991) and of the lightest, high M/L ratio, stars (Capaccioli et al. 1993b).

Dynamical models based on the assumption of constant M/L ratios give in most cases a reasonable description of the observed data. A detailed review of the various techniques is given in Bertin and Stiavelli (1992) and we refer to this work for a comprehensive summary.

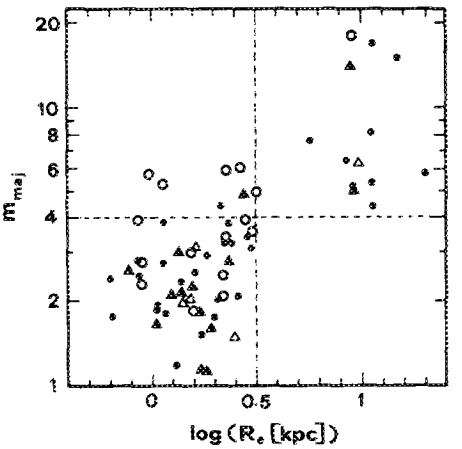

Fig. 12. Trend of the n parameter in the modified de Vaucouleurs law as a function of the logarithm of the effective radius for a sample of ellipticals in Fornax and Virgo (from Caon et al. 1993). • E Virgo; △, SO Virgo; ○ E Fornax; △, SO Fornax

Here we want to stress that if kinematical data extend over a relatively large in effective radii, contradicting results are obtained due to the interplaying roles of anisotropy and variable M/L ratios.

9.4 Specific angular momentum

The specific angular momentum $j = J/M$ of spheroidal galaxies is usually estimated by means of the maximum rotational velocity V_{max} and of the effective radius R_e: $J/M = R_e \times V_{max}$ (e.g. Mineva 1988). An approach which, besides the usual intrinsic geometry arguments (i.e. unknown intrinsic structure and viewing angle) is also undermined by the fact that V_{max} is not known for most elliptical galaxies. Following a different approach, Busarello et al. (1994a) have derived j within r_e for a sample of 62 ellipticals. Their results confirm that also early-type systems follow the $j \propto M^{\frac{2}{3}}$ relation known to hold over several magnitudes in mass (Brosche 1973) even though j is, on average, $\sim 1/6$ of the average value for spiral galaxies (Capaccioli 1973, Bertola and Capaccioli 1975, 1978; Fall 1983). Disky ellipticals and lenticulars tend to fill the gap between spheroidal systems and spirals (Busarello et al. 1994a).

The lower value of j for spheroidal systems implies that some angular momentum must have been dissipated either at an early phase of formation – tidal stripping of the external regions of protogalaxies, angular momentum transfer from the luminous to dark matter (Fall 1983, Barnes and Efstathiou 1987, Curir et al. 1993) – or at later stages by means of hierarchical merging (Hernquist 1993, and references therein).

Another quantity which is related to j is the so-called *'spin parameter'* defined as $\lambda = (j|E|^{\frac{1}{2}})(GM)$ (Peebles 1971), where G is the gravitational constant, M is the mass and E is the total energy per unit of mass. On average, disky ellipticals and lenticulars have $\lambda > 0.05$ (Busarello et al. 1994a), in good agreement with the results of N–body simulations (Barnes and Efstathiou 1987). The spin parameter also correlates with the mass: $\lambda \propto M^{-0.16\pm0.06}$ which, compared to the results of N–body simulations of dissipationless collapse, $\lambda \propto M^{-0.03}$, confirms that some dissipative

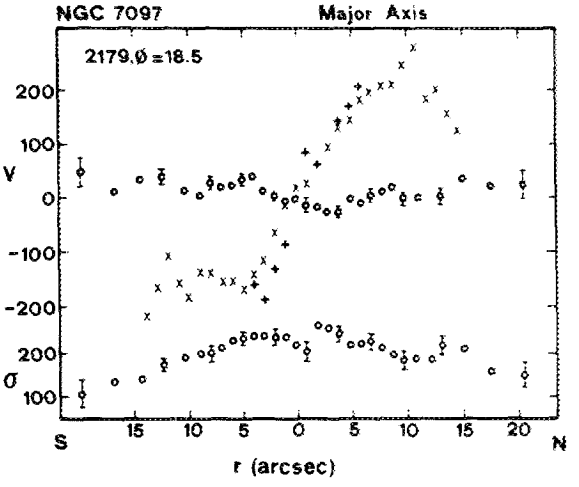

Fig. 13. Major axis rotation curve for the E4 galaxy NGC 7097 from gas ([OII] = cross, [OIII] = plus) and stars (*open circles*), and the stellar velocity dispersion profile (from Caldwell et al. 1986). The decoupling is striking and is consistent with the gas forming a centrally concentrated disk inclined at 60° with respect to the line of sight

process must have occurred during the formation phase (Curir et al. 1993; Barnes and Efstathiou 1987).

9.5 Metallicity

Even though the study of the correlations between average metallicities, metallicity gradients, and kinematical properties, is still in an embryonic stage, some conclusions can already be drawn.

Metal abundances, as measured in elliptical galaxies by the Mg2 index, increase with both luminosity and central velocity dispersion (Gorgas et al. 1990, Bender 1992, Danziger et al. 1993b). There seems to be no correlation between the metallicity and the velocity dispersion gradients (Danziger et al. 1993b). The existence of a correlation between mass (or luminosity) and metallicity gradient is expected on the basis of dissipative galaxy formation models (Larson 1974, Matteucci and Tornambé 1987, and references therein). According to Danziger et al. (1993b) – even though their conclusions should be regarded as preliminary due to insufficient statistics – the existence of correlations of metallicity gradient with total mass, as well as with V_{max}, flattening, and anisotropy parameter, are strongly dependent on the sample selection: all correlations being strengthened (in the direction predicted by the dissipative formation models) by restricting the sample to lenticulars or to low luminosity objects only.

If only giant ellipticals are taken into account, no correlation is found, thus suggesting that they have formed via different mechanisms. These findings are in agreement with the above mentioned segregation observed in the $(\mu_e, \log R_e)$ plane and support the suggestion that giant ellipticals are the result of mergers (White 1980, Capaccioli et al. 1992, 1993a). There is a quite tight correlation between the position of a galaxy

in the (Mg2, σ_0) plane and the degree of morphological disturbance (Schweizer et al. 1990).

Acknowledgements. We wish to thank Drs. M. Arnaboldi, R. Assendorp, G. Busarello, S. Capozziello, G. Djorgovski, S. Odehwan, K.-H. Schmidt, M. Stiavelli, and M. Vietri for criticizing a preliminary version of the manuscript.

References

Amico P., Bertin G., Bertola F., Buson L.M., Danziger I.J., Dejonghe H., Pizzella A., Sadler E.M., Stiavelli M., Saglia R.P., de Zeeuw P.T., Zeilinger W.W.: 1993, in *Structure, Dynamics, and Chemical Evolution of Elliptical Galaxies*, eds. I.J. Danziger, W.W. Zeilinger, K. Kjär, ESO: Munich, p. 225
Arnaboldi M., Capaccioli M., Barbaro G., Buson L., Longo G.: 1993b, *A&A*, 268, 103
Arnaboldi M., Capaccioli M., Cappellaro E., Held E.V., Sparke L.: 1993a, *A&A*, 267, 21
Arnaboldi M., Capaccioli M., Combes F.: 1993c, *Mount Stromlo Prepr.*
Arnaboldi M., Sparke L.S.: 1994, *AJ*, 107, 958
Courtes G., Georgelin Y., Bacon R., Monet G., Boulesteix J.: 1988, in *Instrumentation for Ground Based Optical Astronomy. Present and Future*, ed. L. Robinson, Springer: N.Y., p. 266
Bacon R., Monnet G., Simien F.: 1985, *Afz*, 23, 396
Balcells M.: 1992, in *Morphological and Physical Classification of Galaxies*, eds. G. Longo, M. Capaccioli, G. Busarello, Kluwer: Dordrecht, p. 221
Balcells M., Carter D.: 1993, *A&A*, 279, 376
Balcells M., Quinn P.J.: 1990, *ApJ*, 361, 381
Balcells M., Stanford S.A.: 1990, *ApJ*, 362, 443
Barbon R., Benacchio L., Capaccioli M.: 1976, *A&A*, 51, 25
Barnes J., Efstathiou G.: 1987, *ApJ*, 319, 575
Baum S.A., Heckman T., van Bruegel W.: 1989, *ESO Workshop on 'Extranuclear Activity'*, eds. E.J.A. Meurs, R.A.E. Fosbury, ESO: Munich, p. 37
Bender R.: 1988a, *A&AL*, 193, L7
Bender R.: 1988b, *A&AL*, 202, L5
Bender R.: 1990a, in *Dynamics and Interactions of Galaxies*, ed. R. Wielen, Springer: Berlin, p. 232
Bender R.: 1990b, *A&A*, 229, 441
Bender R.: 1992, in *IAU Symp. No. 149 'The Stellar Properties of Galaxies'*, eds. B. Barbuy, A. Renzini, Reidel: Dordrecht, p. 267
Bender R., Capaccioli M., Macchetto F., Nieto J.-L., et al.: 1993, in *Structure, Dynamics, and Chemical Evolution of Elliptical Galaxies*, eds. I.J. Danziger, W.W. Zeilinger, K. Kjär, ESO: Munich, p. 3
Bender R., Möllenhoff C.: 1987, *A&A*, 177, 71
Bender R., Nieto J.-L.: 1990, *A&A*, 239, 97
Bender R., Paquet A., Nieto J.-L.: 1991, *A&A*, 246, 349
Bender R., Surma P.: 1992, *A&A*, 258, 250
Bender R., Surma P., Döbereiner, S., Möllenhoff C., Madejsky R.: 1989, *A&A*, 217, 35
Bertin G.: 1993, in *Structure, Dynamics, and Chemical Evolution of Elliptical Galaxies*, eds. I.J. Danziger, W.W. Zeilinger, K. Kjär, ESO: Munich, p. 243
Bertin G., Saglia R.P., Stiavelli M.: 1988, *ApJ*, 330, 78
Bertin G., Stiavelli M.: 1993, *Rep. Progr. Phys.*, 56, 493
Bertola F.: 1987, in *IAU Symp. No. 127 'Structure and Dynamics of Elliptical Galaxies'*, ed. T. de Zeeuw, Kluwer: Dordrecht, p. 135
Bertola F., Bettoni D., Capaccioli M.: 1983, in *IAU Symp. No 100 'Internal Kinematics and Dynamics of Stellar Systems'*, ed. E. Athanassoula, Reidel: Dordrecht, p. 311
Bertola F., Bettoni D., Danziger I.J., Sadler E.M., Sparke L.S., de Zeeuw P.T.: 1991, *ApJ*, 373, 369
Bertola F., Buson L., Zeilinger W.W.: 1992, *ESO Prepr.*, No. 881
Bertola F., Capaccioli M.: 1975, *ApJ*, 200, 439
Bertola F., Capaccioli M.: 1978, *ApJL*, 219, L95
Bertola F., Galletta G., Zeilinger W.W.: 1985, *ApJL*, 292, L51
Bettoni D., Galletta G., Oosterloo T.: 1991, *MNRAS*, 248, 544

Bicknell G.V., Carter D., Killeen N.E., Bruce T.E.: 1989, *ApJ*, 336, 639
Binggeli B.: 1980, *A&A*, 82, 289
Binggeli B., Sandage A., Tarenghi M.: 1984, *AJ*, 89, 64
Binney J.J.: 1976, *MNRAS*, 177, 19
Binney J.J.: 1978, *MNRAS*, 183, 501
Binney J.J.: 1985, *MNRAS*, 212, 767
Binney J.J., Mamon G.S.:1982, *MNRAS*, 200, 361
Binney J.J., Tremaine S.:1987, *Galactic Dynamics*, Princeton: Princeton Univ. Press
Blackman C.P., Wilson A.S., Ward M.J.: 1983, *MNRAS*, 202, 1001
Bland J., Taylor K., Atherton P.D.: 1987, *MNRAS*, 228, 595
Bottema R.: 1988, *A&A*, 197, 105
Brault J.M., White D.R.: 1971, *A&A*, 13, 169
Brosche P.: 1973, *ZsAp*, 57, 143
Burbidge E.M., Burbidge G.R., Fish R.A.: 1961a, *ApJ*, 133, 393
Burbidge E.M., Burbidge G.R., Fish R.A.: 1961b, *ApJ*, 133, 1092
Burbidge E.M., Burbidge G.R., Fish R.A.: 1961c, *ApJ*, 134, 251
Burstein D., Bender R., Faber S.M., 1993, in *Structure, Dynamics, and Chemical Evolution of Elliptical Galaxies*, eds. I.J. Danziger, W.W. Zeilinger, K. Kjär, ESO: Munich, p. 31
Busarello G., Longo G., Di Martino F.: 1989, *Atlas of Velocity Dispersion Profiles and Rotation Curves for Elliptical and Lenticular Galaxies*, Liguori: Napoli
Busarello G., Longo G., Feoli A.: 1992, *A&A*, 262, 52
Busarello G., Longo G., Feoli A.: 1994a, in preparation
Busarello G., Longo G., Rifatto A.: 1994b, *Astr. Nach.*, in press
Caldwell N., Kirshner R.P., Richstone D.O.: 1986, *ApJ*, 305, 136
Caon N., Capaccioli M., D'Onofrio M.: 1993, *MNRAS*, in press
Capaccioli M.: 1973, in *Giornate Copernicane ed Atti del Convegno di Cima Ekar* (Asiago), eds. L. Rosino, C. Barbieri, Astron. Obs.: Padova, p. 101
Capaccioli M.: 1979, in *Photometry, Kinematics, and Dynamics of Galaxies* (Austin), ed. D.S. Evans, The University of Texas Press: Austin, p. 165
Capaccioli M.: 1987, in *IAU Symp. No. 127 'Structure and Dynamics of Elliptical Galaxies'*, ed. T. de Zeeuw, Kluwer: Dordrecht, p. 47
Capaccioli M.: 1989, in *The World of Galaxies* (Paris), eds. H. Corwin, L. Bottinelli, Springer: Heidelberg, p. 208
Capaccioli M., Caon N.: 1991, *MNRAS*, 248, 523
Capaccioli M., Caon N.: 1992, in *Morphological and Physical Classification of Galaxies*, eds. G. Longo, M. Capaccioli, G. Busarello, Kluwer: Dordrecht, p. 99
Capaccioli M., Caon N., D'Onofrio M.: 1992, *MNRAS*, 259, 323
Capaccioli M., Caon N., D'Onofrio M.: 1993b, in *Structure, Dynamics, and Chemical Evolution of Elliptical Galaxies*, eds. I.J. Danziger, W.W. Zeilinger, K. Kjär, ESO: Munich, p. 43
Capaccioli M., Caon N., Rampazzo R.: 1990b, *MNRAS*, 242, 24p
Capaccioli M., Cappellaro E. Held E.V., Vietri M.: 1993a, *A&A*, 274, 69
Capaccioli M., de Vaucouleurs G.: 1983, *ApJS*, 52, 465
Capaccioli M., Fasano G., Lake G.: 1984, *MNRAS*, 209, 317
Capaccioli M., Held V.E., Lorenz H., Vietri M.: 1990a, *AJ*, 99, 1813
Capaccioli M., Longo G.: 1990, in *Windows on Galaxies*, eds. G. Fabbiano, J.S. Gallagher, A. Renzini, Kluwer: Dordrecht, p. 23
Cappellaro E., Capaccioli M., Held V.E.: 1989, *The Messenger*, 58, 48
Cappellaro E., Capaccioli M., Held V.E.: 1990, in *Bulges of Galaxies*, eds. B.J. Jarvis, D.M. Terndrup, ESO: Munich, p. 227
Carollo C.M., Danziger I.J.: 1993, in *Structure, Dynamics, and Chemical Evolution of Elliptical Galaxies*, eds. I.J. Danziger, W.W. Zeilinger, K. Kjär, ESO: Munich, p. 431
Carter D.: 1987, *ApJ*, 312, 514
Carter D., Efstathiou G., Ellis R.S., Inglis I, Godwin J.: 1981 *MNRAS*, 195, 15P
Carter D., Inglis I., Ellis R.S., Efstathiou G., Godwin J.: 1985, *MNRAS*, 212, 471
Carter D., Jenkins C.R., 1993, *MNRAS*, 263, 1049
Carter D., Sadler E.M.: 1990, *MNRAS*, 245, 12
Ciarduilo R., Jacoby G.H., Dejonghe H.B.: 1993, *ApJ*, 414, 454

Cinzano P.A., van der Marel R.P.: 1993, in *Structure, Dynamics, and Chemical Evolution of Elliptical Galaxies*, eds. I.J. Danziger, W.W. Zeilinger, K. Kjär, ESO: Munich, p. 79
Combes F., Braine J., Casoli F., Gerin M., van Driel W.: 1992, *A&A*, 259, L65
Contopoulos G.: 1956, *ZsAp*, 39, 126
Curir A., De Felice F., Busarello G., Longo G.: 1993, *Ap. Lett. & Comm.*, 28, 323
Dalle Ore C., Faber S.M., Jesus J., Stoughton R., Burstein D.: 1991, *ApJ*, 366, 38
Danziger I.J., Carollo C.M., Buson L., Matteucci F., Brocato E.: 1993b, in *Structure, Dynamics, and Chemical Evolution of Elliptical Galaxies*, eds. I.J. Danziger, W.W. Zeilinger, K. Kjär, ESO: Munich, p. 399
Danziger I.J., Zeilinger W.W., Kjär K.: 1993a, editors *Structure, Dynamics, and Chemical Evolution of Elliptical Galaxies*, ESO Conf. and Work. Proc. No. 45, ESO: Munich
Davies R.L.: 1981, *MNRAS*, 194, 879
Davies R.L., Birkinshaw M.: 1988, *ApJS*, 68, 409
Davies R.I., Efstathiou G., Fall S.M., Illingworth G., Schechter P.L.: 1983, *ApJ*, 266, 41
Davies R.I, Illingworth G.: 1986, *ApJ*, 302, 234
Davoust E., Paturel G., Vauglin I.: 1985, *A&AS*, 61, 273
Demoulin–Ulrich M.H., Butcher H.R., Boksemberg A.: 1984, *ApJ*, 285, 527
de Vaucouleurs G.: 1948a, *Ann. d'Ap*, 11, 267
de Vaucouleurs G.: 1948b, *Compte Rendus*, 227, 548
de Vaucouleurs G.: 1953, *MNRAS*, 113, 134
de Vaucouleurs G., Capaccioli M.: 1979, *ApJS*, 40, 699
Dejonghe H.: 1987a, *MNRAS*, 224, 13
Dejonghe H.: 1987b, *ApJ*, 320, 477
de Zeeuw T.: 1987, editor, *IAU Symp. No. 127 'Structure and Dynamics of Elliptical Galaxies'*, Reidel: Dordrecht
de Zeeuw T., Franx M.: 1991, *ARA&A*, 29, 239
Djorgovski S.: 1993 in *The Globular Cluster–Galaxy Connection*, eds. J. Brodie, D. Smith, A.S.P. Conference Series, in press
Djorgovski S.: 1994, in *Ergodic Concepts in Stellar Dynamics*, eds. D. Pfenniger, V.G. Gurzadyan, Springer: Heidelberg, in press (*Caltech Astrophys. Prepr.*)
Djorgovski S., Davis M.: 1987, *ApJ*, 313, 59
Djorgovski S., Santiago B.X.: 1993, in *Structure, Dynamics, and Chemical Evolution of Elliptical Galaxies*, eds. I.J. Danziger, W.W. Zeilinger, K. Kjär, ESO: Munich, p. 59
Dressler A.: 1979, *ApJ*, 231, 659
Dressler A.: 1984, *ApJ*, 286, 97
Dressler A., Lynden–Bell D., Burstein D., Davies R.L., Faber S.M., Terlevich R.J., Wegner G.: 1987, *ApJ*, 313, 42
Dressler A., Richstone D.O.: 1988, *ApJ*, 324, 701
Dressler A., Richstone D.O.: 1990, *ApJ*, 348, 120
Duncan M.J., Wheeler J.C.: 1980, *ApJ*, 237, L27
Efstathiou G., Ellis R.S., Carter D.: 1982, *MNRAS*, 201, 975
Faber S.M., Dressler A., Davies R.L., Burstein D., Lynden–Bell D., Terlevich R., Wegner G.: 1987, in *Nearly Normal Galaxies from the Planck Time to the Present*, ed. S.M. Faber, Springer: N.Y., p. 175
Faber S.M., Gallagher J.S.: 1979, *ARA&A*, 17, 135
Faber S.M., Jackson R.E.: 1976, *ApJ*, 204, 668
Fall S.M.: 1983, in *IAU Symp. No 100 'Internal Kinematics and Dynamics of Stellar Systems'*, ed. E. Athanassoula, Reidel: Dordrecht, p. 391
Ferrario M.: 1990, Laurea Thesis, Padova University
Fish R.A.: 1964, *ApJ*, 139, 284
Fisher D., Illingworth G., Franx M.: 1993, in preparation
Forman W., Jones C., Tucker W.: 1985, *ApJ*, 293, 102
Franx M.: 1990, in *Galactic Models*, eds. J.R. Buchler, New York Science Academy: N.Y., p. 67
Franx M.: 1992, in *Morphological and Physical Classification of Galaxies*, eds. G. Longo, M. Capaccioli, G. Busarello, Kluwer: Dordrecht, p. 23
Franx M.: 1993, *IAU Symp. No. 153 'Galactic Bulges'*, eds. H. Dejonghe, H. Habing, Kluwer: Dordrecht, in press
Franx M., Illingworth G.D.: 1988, *ApJL*, 327, L55
Franx M., Illingworth G.D., de Zeeuw T.: 1991, *ApJ*, 383, 112

Franx M., Illingworth G.D., Heckman T.M.: 1989, *ApJ*, 344, 613
Freeman K.C.: 1975, in *Stars and Stellar Systems*, Vol. IX, *Galaxies and the Universe*, eds. A. Sandage, M. Sandage & J. Kristian, Chicago University Press: Chicago, p. 409
Gerhard O.E.: 1983, *MNRAS*, 203, 19p
Gerhard O.E.: 1987, in *IAU Symp. No. 127 'Structure and Dynamics of Elliptical Galaxies'*, ed. T. de Zeeuw, Kluwer: Dordrecht, p. 241
Gerhard O.E.: 1989, in *Dynamics of Dense Stellar Systems*, ed. D. Merritt, Cambridge University Press: Cambridge, p. 61
Gerhard O.E.: 1993, in *Structure, Dynamics, and Chemical Evolution of Elliptical Galaxies*, eds. I.J. Danziger, W.W. Zeilinger, K. Kjär, ESO: Munich, p. 311
Gorgas J., Efstathiou G., Aragon–Salamanca A.: 1990, *MNRAS*, 245, 217
Gott, J.R.: 1975, *ApJ*, 201, 296
Guzman R., Lucey J.R., Bower R.G.: 1993, in *Structure, Dynamics, and Chemical Evolution of Elliptical Galaxies*, eds. I.J. Danziger, W.W. Zeilinger, K. Kjär, ESO: Munich, p. 19
Hamabe M., Kormendy J.: 1987, in *IAU Symp. No. 127 'Structure and Dynamics of Elliptical Galaxies'*, ed. T. de Zeeuw, Kluwer: Dordrecht, p. 379
Harris H.C., Harris G.L.H., Hesser J.E., 1988, in *Globular Cluster systems in Galaxies*, eds. J.E. Grindlay & A.G.D. Philip, Kluwer:Dordrecht, p.205
Hawarden T.G., Elson R.A.W., Longmore A.J., Tritton S.B., Corwin, H.G.: 1981, *MNRAS*, 196, 747
Held E.V., Mould J.R., de Zeeuw T.: 1990, *AJ*, 100, 415
Hernquist L.: 1993, *ApJ*, 409, 548
Hes R., Peletier R.F.: 1992, *ESO Prepr.*, No. 875
Hui X., Ford H.C., Freeman K.C., Dopita M.A.: 1993, *Prepr.*
Illingworth G.D.: 1977, *ApJL*, 218, L43
Illingworth G.D., Franx M.: 1989 in *Dynamics of Dense Stellar Systems*, ed. D. Merritt, Cambridge University Press: Cambridge, p.13
Jarvis B.J., Dubath P.: 1988, *A&A*, 201, L33
Jedrzejewski R.I.: 1987, in *IAU Symp. No. 127 'Structure and Dynamics of Elliptical Galaxies'*, ed. T. de Zeeuw, Kluwer: Dordrecht, p. 37
Jedrzejewski R.I., Schechter P.L.: 1989, *AJ*, 98, 147
Katz N., Richstone D.O.: 1985, *ApJ*, 296, 331
King I.R.: 1966, *AJ*, 71, 64
King I.R.: 1978, *ApJ*, 222, 1
Knapp G.R., Gallagher J.S., Faber S.M.: 1978, *AJ*, 83, 189
Kondrat'ev B.P., Ozernoy L.M.: 1979: *SvAL*, 5, 37
Kormendy J.: 1977, *ApJ*, 218, 333
Kormendy J.: 1984a, *ApJ*, 286, 116
Kormendy J.: 1984b, *ApJ*, 287, 577
Kormendy J.: 1985, *ApJL*, 292, L9
Kormendy J.: 1987, in *IAU Symp. No. 127 'Structure and Dynamics of Elliptical Galaxies'*, ed. T. de Zeeuw, Kluwer: Dordrecht, p. 17
Kormendy J.: 1988a, *ApJ*, 335, 40
Kormendy J.: 1988b, *ApJ*, 325, 128
Kormendy J., Djorgovski S.: 1989, *ARA&A*, 27, 235
Kormendy J., Illingworth G.: 1982, *ApJ*, 256, 481
Kormendy J., Richstone D.: 1992, *ApJ*, 393, 559
Kormendy J., Stauffer J.: 1987, in *IAU Symp. No. 127 'Structure and Dynamics of Elliptical Galaxies'*, ed. T. de Zeeuw, Kluwer: Dordrecht, p. 405
Kormendy J., Westphal D.J.: 1989, *ApJ*, 338, 752
Larsen N., Nörgaard-Nielsen H.U., Kjaergaard P., Dickens R.J.: 1983, *A&A*, 117, 257
Larson R.B.: 1974, *MNRAS*, 166, 585
Larson R.B.: 1975, *MNRAS*, 173, 631
Lauer T.R.: 1985, *MNRAS*, 216, 429
Leach R.: 1981, *ApJ*, 248, 485
Laird I.B., Levison H.F.: 1985, *AJ*, 90, 2652
Lees J.F.: 1991, in *Warped disks and inclined rings around galaxies*, eds. S. Casertano, F. Briggs, P. Sackett, Cambridge University Press: Cambridge, p. 50
Liller M.: 1960, *ApJ*, 132, 306

Liller M.: 1966, *ApJ*, 146, 28
Longo G., Busarello G., Richter G., Zaggia S.: 1993, *A&A*, 282, 411
Longo G., Capaccioli M., Busarello G.: 1992, editors *Morphological and Physical Classification of Galaxies*, Kluwer: Dordrecht
Lowenstein M.: 1992, *ApJ*, 384, 474
Macchetto F., Sparks W.B.: 1992, in *Morphological and Physical Classification of Galaxies*, eds. G. Longo, M. Capaccioli, G. Busarello, Kluwer: Dordrecht, p. 191
Malin D.F.: 1979, *Nature*, 277, 279
Matteucci F., Tornambé A.: 1987, *A&A*, 185, 51
Mellier Y., Mathez G.: 1987, *A&A*, 175, 1
Merritt D.R.: 1982, *AJ*, 87, 1279
Merritt D.R.: 1992, editor, *Dynamics of Dense Stellar Systems*, Cambridge University Press:Cambridge
Merritt D.R.: 1993, in *Structure, Dynamics, and Chemical Evolution of Elliptical Galaxies*, eds. I.J. Danziger, W.W. Zeilinger, K. Kjär, ESO: Munich, p. 275
Merritt D.R., Tremblay B.: 1993, *AJ*, 106, 2229
Merritt D.R., de Zeeuw T.: 1983, *ApJL*, 267, L19
Michard R., 1984, *A&AL*, 140, 39
Michard R., Marchal J.: 1993, in *Structure, Dynamics, and Chemical Evolution of Elliptical Galaxies*, eds. I.J. Danziger, W.W. Zeilinger, K. Kjär, ESO: Munich, p. 257
Michard R., Nieto J.–L.: 1991, *A&AL*, 243, L17
Mineva V.A.: 1988, *SvA*, 32, 366
Minkowski R.: 1954, *Carnegie Inst. Year Book*, No. 53, 26
Minkowski R.: 1961 in *IAU Symp. No. 15 'Problems of Extragalactic Research'*, ed. G.C. McVittie, MacMillan: N.Y., p. 112
Morton D.C., Thuan T.X., 1973, *ApJ*, 180, 705
Morton D.C., Elmegreen B.G., 1976, *ApJ*, 205, 63
Morton D.C., Chevalier R.A.: 1972, *ApJ*, 174, 489
Mould J.R., Oke J.B., de Zeeuw P.T., Nemec J.M.: 1990, *AJ*, 99, 1823
Nicholson R.A., Bland-Hawthorn J., Taylor K.: 1992, *ApJ*, 387, 503
Nieto J.-L.: 1988, *Bul. Academia Nacional de Ciencias de Cordoba*, 58, 239
Nieto J.-L., Capaccioli M., Held V.E.: 1988, *A&AL*, 195, L1
Norman C.A., May A., van Albada T.S.: 1985, *ApJ*, 296, 20
Peebles P.J.: 1971, *A&A*, 11, 377
Pesce E., Capuzzo–Dolcetta R., Vietri M.: 1992, *MNRAS*, 254, 466
Peterson R., Caldwell N.: 1993, *AJ*, 105, 1411
Quillen A.C., de Zeeuw P.T., Phinney E.S., Phillips T.G.: 1991, *Prepr.*
Richstone D.O., Bower G., Dressler A.: 1990, *ApJ*, 353, 118
Richstone D., Sargent W.L.W.: 1972, *ApJ*, 176, 91
Richter G., Longo G., Lorenz H., Zaggia S.: 1992, *The Messenger*, 68, 48
Rix H.–W., White S.D.M.: 1990, *ApJ*, 362, 52
Rix H.–W., White S.D.M.: 1992, *MNRAS*, 254, 389
Roberts M.S., Hogg D.E., Bregman J.N., Forman W.R., Jones C.: 1991, *ApJS*, 75, 751
Rubin V.C., Graham J.A., Kenney J.D.P.: 1992, *ApJL*, 349, L9
Sadler E.M., Gerhard O.E.: 1985 in *New Aspects of Galaxy Photometry* (Toulouse), ed. J.-L. Nieto, Springer: N.Y., p. 269
Sackett P.D., Sparke L.S.: 1990, *ApJ*, 361, 408
Saglia R.P., Bender R., Dressler A.: 1993b, *A&A*, 279, 75
Saglia R.P., Bertin G., Bertola F., Danziger I.J., Dejonghe H., Sadler E.M., Stiavelli M., de Zeeuw P.T., Zeilinger W.W.: 1993a, *ApJ*, 403, 567
Sandage R.A.: 1972, *ApJ*, 176, 21
Sandage A., Visvanathan N.: 1978, *ApJ*, 223, 707
Sarazin C.L.: 1986, *Rev. Mod. Phys.*, 58, 1
Sargent W.L.W., Schechter P.L., Boksemberg A., Shortridge K.: 1977, *ApJ*, 212, 326
Sargent W.L.W., Young P.J., Boksemberg A., Shortridge K., Lynds C.R., Hartwick F.D.A.: 1978, *ApJ*, 22, 731
Schechter P.L., Sancisi R., van Woerden H., Lynds C.R.: 1984, *MNRAS*, 208, 111
Schwarzschild M.: 1979, *ApJ*, 232, 236
Schweizer F., Seitzer P., Faber S.M., Burstein D., Dalle Ore C.M., Gonzalez J.J.: 1990, *ApJL*, 364, L33

Schweizer F., van Gorkom J.H., Seitzer P.: 1989, *ApJ*, 338, 770
Schweizer F., Whitmore B.C., Rubin V.C.: 1983, *AJ*, 88, 909
Schweizer F., van Gorkom J.H., Seitzer P.: 1989, *ApJ*, 338 770
Sharples R.M.: 1988, in *Globular Cluster Systems in Galaxies*, eds. J.E. Grindlay, A.G.D. Philip, Kluwer: Dordrecht, p. 545
Simien F., de Vaucouleurs G.: 1986, *ApJ*, 302, 564
Simkin S.M.: 1972, *Nature*, 239, 43
Simkin S.M.: 1974, *A&A*, 31, 129
Sparke L.S.: 1986, *MNRAS*, 219, 657
Stanford S., Balcells M.: 1990, *ApJ*, 355, 59
Stark A.A.: 1977, *ApJ*, 213, 368
Steiman–Cameron T.Y., Durisen R.H.: 1982, *ApJL*, 263, L51
Steiman–Cameron T.Y., Durisen R.H.: 1988, *ApJ*, 325, 26
Steiman–Cameron T.Y., Kormendy J., Durisen R.H.: 1992, *AJ*, 104, 1339
Stiavelli M., Londrillo P., Messina A.: 1991, *MNRAS*, 251, 57p
Tenjes P., Busarello G., Longo G., Zaggia S.: 1993, *A&A*, 275, 61
Terlevich R., Davies R., Faber S.M., Burstein D.: 1981, *MNRAS*, 193, 38
Tholine J.E., Durisen R.H.: 1982, *ApJ*, 257, 94
Thomas P.A.: 1986, *MNRAS*, 220, 951
Tonry J.L.: 1984, *ApJ*, 283, L27
Tonry J.L.: 1987, *ApJ*, 322, 632
Tonry J.L., Davis M.: 1979, *AJ*, 84, 1511
Toomre A.: 1977, in *The Evolution of Galaxies and Stellar Populations* (Yale), eds. B.M. Tinsley, R.B. Larson, Yale Univ. Observ: New Haven, p. 401
Trinchieri G., Di Serego S.: 1991, *AJ*, 101, 1647
van Albada T.S., Kotanyi C.G., Schwarzschild M.: 1982, *MNRAS*, 198, 303
van den Bergh S.: 1990, in *The Evolution of the Universe of Galaxies. Edwin Hubble Centennial Symp.*, ed. R.G. Kron, *Astron. Soc. Pac. Conf. Ser.*, 10, p. 70
van der Marel R.P.: 1991, *MNRAS*, 253, 710
van der Marel R.P., Binney J.J., Davies R.L.: 1990, *MNRAS*, 245, 582
van der Marel R.P., Franx M.: 1993, *ApJ*, 407, 525
van Gorkom J.H.: 1992, in *Morphological and Physical Classification of Galaxies*, eds. G. Longo, M. Capaccioli, G. Busarello, Kluwer: Dordrecht, p. 233
van Gorkom J.H., Knapp G.R., Raimond E., Faber S.M., Gallagher J.S.: 1986, *AJ*, 91, 791
van Gorkom J.H., van der Hulst J.M., Hanish A.D., Tubbs A.D.: 1990 *AJ*, 99, 1781
van Houten J.C.: 1961, BAN, 16,1
Vietri M.: 1986, *ApJ*, 306, 48
Wagner S.J.: 1990, in *Dynamics and Interactions of Galaxies*, ed. R. Wielen, Springer: Berlin, p. 244
Wagner S.J., Bender R., Möllenhof C.: 1988, *A&AL*, 195, L5
Wakamatsu r.–I.: 1993, *AJ*, in press
White S.D.M.: 1980, *MNRAS*, 190, 1p
Whitmore B.C.: 1991, in *Warped disks and inclined rings around galaxies*, eds. S. Casertano, F. Briggs, P. Sackett, Cambridge University Press: Cambridge, p. 60
Whitmore B.C., Lucas R.A., McElroy B.D., Steiman–Cameron T.Y., Sackett P.D., Olling R.P.: 1990, *AJ*, 100, 1489
Whitmore B.C., Mc Elroy D., Schweizer F.: 1987, in *IAU Symp. No. 127 'Structure and Dynamics of Elliptical Galaxies'*, ed. T. de Zeeuw, Kluwer: Dordrecht, p. 413
Wielen R.: 1990, editor *Dynamics and Interactions of Galaxies*, Springer: Berlin
Wilkinson A., Sharples R.M., Fosbury R.A.E., Wallace P.T.: 1986, *MNRAS*, 218, 297
Williams T.B., Schwarzschild M.: 1979, *ApJ*, 227, 56
Wilson C.P.: 1975, *AJ*, 80, 175
Winsall M.L., Freeman K.C.: 1993, in *Structure, Dynamics, and Chemical Evolution of Elliptical Galaxies*, eds. I.J. Danziger, W.W. Zeilinger, K. Kjär, ESO: Munich, p. 87
Wyse R.F., Jones B.J.T., 1984, *ApJ*, 286, 88
Young P.J., Westphal J.A., Kristian J., Wilson C.D., Landauer F.P.: 1978, *ApJ*, 221, 721
Zepf S., Whitmore B.C., Levison H.F.: 1991, *ApJ*, 383, 524